Mutation of the Follicle-Stimulating Hormone Receptor Gene 5′-Untranslated Region Associated With Female Hypertension

Tomohiro Nakayama, Nobuhiro Kuroi, Morihiko Sano, Yasuharu Tabara, Tomohiro Katsuya, Toshio Ogihara, Yoshio Makita, Akira Hata, Michiko Yamada, Norio Takahashi, Nobuhito Hirawa, Satoshi Umemura, Tetsuro Miki, Masayoshi Soma

Abstract—Inactivating mutations in the follicle-stimulating hormone receptor (FSHR) gene have been reported to cause hereditary hypergonadotropic ovarian failure. It has been found recently that the FSHR knockout mouse exhibits hypertension. The aim of the present study was to investigate the association between polymorphisms in the human FSHR gene and essential hypertension (EH) by using single nucleotide polymorphisms (SNPs). We selected 5 SNPs in the gene (rs1394205, rs2055571, rs11692782, rs1007541, and rs2268361) and performed 2 genetic case–control studies in different populations. A confirmative case–control study was performed using 1035 EH patients and 1058 age-matched controls. Transcriptional activities were measured with a luciferase assay system. The first case–control study found that the A allele of rs1394205 was significantly higher in EH females (P=0.010). In addition, in the confirmative case–control study, there was a significant difference for this SNP between female normotensive subjects (44.5%) and EH patients (50.7%) (P=0.043). Multiple logistic regression analysis in female subjects also revealed a significant association of subjects with the A allele of rs1394205 with EH (P=0.033), with the odds ratio calculated as 1.68 (95% CI: 1.04 to 2.73). Transcriptional activity of the A allele was 56±8% (mean±SD) of that observed for the G-type allele (P=0.001). Serum estradiol levels were significantly lower in patients with the A/A genotype than in patients without the A/A genotype (P=0.004). The SNP in the 5′-untranslated region of the FSHR gene affects levels of transcriptional activity and is a susceptibility mutation of EH in women. (***Hypertension.* 2006;48:512-518.**)

Key Words: hypertension, essential ■ hormones ■ case–control studies

It is likely that essential hypertension (EH) is a polygenic disorder that results from the inheritance of a number of susceptibility genes. The causal genes identified may contribute from 30% to 50% of the variations in blood pressure seen among individuals.[1] These genetic determinants interact with environmental factors, such as dietary salt, to produce the final disease phenotype. Despite significant recent progress in genomic and statistical tools, the genetic dissection of human EH remains a major challenge.[2]

The effects of follicle-stimulating hormone (FSH) are mediated by its interaction with specific receptors and the activation of G_s, the stimulatory guanine nucleotide binding protein, which stimulates the enzyme adenylyl cyclase.[3] The FSH receptor (FSHR) belongs to the superfamily of G protein–coupled receptors that are characterized by the common structural feature of 7 transmembrane domains. They differ structurally from other G protein–coupled receptors in that they contain a large extracellular domain in the amino-terminal part of the receptor protein, which is required for interaction with complex glycoprotein hormones.[4–6] The human FSHR gene is localized to 2p21 to p16 and is composed of 10 exons.[7] The 5′-flanking region of the gene has neither a TATA nor a CCAAT box and exhibits promoter-type features that are seen in housekeeping genes.[8]

Inactivating mutations in the FSHR gene have been reported to cause hereditary hypergonadotropic ovarian failure in women.[9] These mutations have been shown to be associated with a recessive inheritance pattern, and all of the affected subjects have homozygous or compound heterozygous mutations in the coding region of the gene. The phenotype in men for

Received December 11, 2005; first decision January 4, 2006; revision accepted June 15, 2006.

From the Division of Molecular Diagnostics (T.N.), Advanced Medical Research Center, and Division of Nephrology and Endocrinology (M.S.), Department of Medicine, Nihon University School of Medicine (N.K., M.S.), Tokyo, Japan; Departments of Basic Medical Research and Education (Y.T.) and Geriatric Medicine (T.M.), Ehime University Graduate School of Medicine, Ehime, Japan; Department of Geriatric Medicine (T.K., T.O.), Osaka University Graduate School of Medicine, Osaka, Japan; Department of Pediatrics (Y.M.), Asahikawa Medical College, Asahikawa, Japan; Department of Public Health (A.H.), Graduate School of Medicine, Chiba University, Chiba, Japan; Departments of Clinical Studies (M.Y.) and Genetics (N.T.), Radiation Effects Research Foundation; and the Department of Medical Science and Cardiorenal Medicine (N.H., S.U.), Yokohama City University Graduate School of Medicine, Yokohama City, Japan.

Correspondence to Tomohiro Nakayama, Division of Molecular Diagnostics, Advanced Medical Research Center, Nihon University School of Medicine, Ooyaguchi-kamimachi, 30-1 Itabashi-ku, Tokyo 173-8610, Japan. E-mail tnakayam@med.nihon-u.ac.jp

Hypertension **is available at http://www.hypertensionaha.org** **DOI: 10.1161/01.HYP.0000233877.84343.d7**

this particular FSHR mutation is less clear, with homozygous men found to have normal masculinization and circulating testosterone, normal or slightly elevated luteinizing hormone (LH), moderately elevated FSH, and slightly to severely reduced testicular volume.[10] Although men with inactivating mutations have abnormal semen parameters that range from severe-to-moderate oligozoospermia, normal sperm concentrations with low volumes, or teratozoospermia (reported in 1 individual), none have been found to be azoospermic, and there are reports of such individuals fathering children. These results suggest that FSHR mutations have a greater consequence in women than in men.

The FSHR knockout mice have ovarian insufficiency, low estrogen levels with functionally responsive estrogen receptors, and increased testosterone levels.[11–13] They also exhibit the same changes seen in postmenopausal women, such as osteoporosis, hypercholesterolemia, and weight gains. In 2003, Javeshghani et al[14] reported that these mice have increased blood pressure, indicating that there is vascular remodeling.

There have been no previous studies on the association between the FSHR gene and EH. The aim of the present study was to investigate the association between the human FSHR gene and EH through the use of single nucleotide polymorphisms (SNPs) in the human FSHR gene.

Methods

First Case–Control Study

Patients and control subjects from the northern area of Tokyo were recruited for the first case–control screening study. A total of 235 patients were diagnosed with EH according to the following criteria: seated systolic blood pressure (SBP) >160 mm Hg and/or diastolic blood pressure (DBP) >100 mm Hg on 3 occasions within 2 months after the first medical examination. None of the patients were using antihypertensive medications, and subjects diagnosed with secondary hypertension were excluded. We also included 237 normotensive (NT) healthy individuals as controls. None of the NT participants had a family history of hypertension, and all had SBP and DBP <130 and 85 mm Hg, respectively. A family history of hypertension was defined as a previous diagnosis of hypertension in grandparents, uncles, aunts, parents, or siblings. Informed consent was obtained from each individual as per a protocol approved by the Human Studies Committee of Nihon University.[15]

Confirmative Case-Control Study: Subgroup Collaboration Study With the Hypertensive Section of the Japanese Millennium Project

For confirmation of a possible SNP association, we used a second set of 1035 EH patients and 1058 age-matched control subjects, who were recruited through a subgroup collaboration study with the hypertensive section of the Japanese Millennium Project. Six medical institutes took part in the collaborative study and collected data on hypertensive cases and controls. Hypertensive patients were defined as having SBP ≥140 mm Hg or DBP ≥90 mm Hg or were patients with chronic antihypertensive medication. To increase the statistical power of the present study, hypertensive subjects additionally had to meet the following criteria: age <60 years old or onset of hypertension <50 years of age, a family history of hypertension, and without obesity (body mass index <26 kg/m^2). The NT criteria were as follows: SBP/DBP <130/85 mm Hg, without a family history of hypertension, and without obesity. In this study, both groups were recruited from throughout Japan, and informed consent was obtained from each individual as per the protocol approved by each institutions' human studies committee.

Biochemical Analysis

Serum concentrations of total cholesterol, triglyceride, high-density lipoprotein cholesterol, uric acid, creatinine, and γ-glutamyl transpeptidase were measured using the methods of the clinical laboratory department of each hospital or institution.

Genotyping

Using information about allelic frequencies of SNPs registered on the web site of the National Center for Biotechnology Information and Celera Discovery System-Applied Biosystems, 5 SNPs with minor allele frequencies >20% were selected. SNPs with relatively high minor allele frequencies have been shown to be very useful as genetic markers for genetic case–control studies.

We examined the association between EH and 5 SNPs in the human FSH receptor gene. All 5 of the SNPs were confirmed using the National Center for Biotechnology Information web site and Applied Biosystems-Celera Discovery System with the accession numbers, rs1394205 (C_426553_10), rs2055571 (C_246842_10), rs11692782 (C_228130_10), rs1007541 (C_9561251_1_), and rs2268361 (C_11813031_1_; Figure 1 a). Genotypes were determined using Assays-on-Demand kits (Applied Biosystems) together with TaqMan PCR.[16] When allele-specific fluorogenic probes hybridize to the template during the PCR, the 5′ nuclease activity of *Taq* polymerase can discriminate alleles. Cleavage results in increased emission of a reporter dye that otherwise is quenched by the dye minor groove binder (MGB). Each 5′ nuclease assay requires 2 unlabeled PCR primers and 2 allele-specific probes. Each probe is labeled with a reporter dye (VIC [a proprietory dye from Applied Biosystems] and 6-carboxyfluorescein [FAM]) at the 5′ end and MGB at the 3′ end. Amplification by PCR preceded using TaqMan Universal Master Mix (PE Biosystems) in a 25-μl reaction volume containing 50 ng of DNA, 700 nM primer, and 100 nM probe final concentrations. Thermal cycling conditions consisted of 95°C for 10 minutes and then 40 cycles of 92°C for 15 s and 60°C for 1 minute in a GeneAmp 9700 system. Fluorescence levels of the PCR products were measured using an ABI PRISM 7700 Sequence Detector (Applied Biosystems), which resulted in 3 genotypes of 2 alleles being clearly identified. We analyzed *cis* elements in the 5′ upstream region of the gene using AliBaba2 software that was obtained from the Biological Databases web site (http://www.gene-regulation.com/pub/programs.html#alibaba2).

Linkage Disequilibrium Analysis

SNPAlyze version 3.2 (DYNACOM Co, Ltd) was used for determining haplotype and linkage disequilibrium (LD) analyses and is available online at http://www.dynacom.co.jp/products/package/snpalyze/index.html (Figure 1b).

Preparation of Plasmids Including the G-Type or A-Type DNA Fragment

G-type and A-type rs1394205 reporter constructs were made. Because it has been reported that the −250-bp upstream region of this gene has a core promoter activity, 2 oligonucleotide primers, 5′-CCTTAGGTCAGGGTGTAAGAAACCC-3′ (bases −202 to −226) and 5′-GGCCATAATTATGCATCCATCCACC-3′ (bases +6 to −19), were designed (Figure 1c).[8] These primers contain the *Kpn*I and *Hin*dIII restriction sites, respectively. After digestion with *Kpn*I and *Hin*dIII, PCR products were subcloned into the *Kpn*I and *Hin*dIII sites of the luciferase reporter gene vector pGV-B2 (Tokyo Ink). The G-type and A-type constructs were verified by sequencing.

Measurement of Transcriptional Activities of G-Type and A-Type Alleles

For transfection of Chinese hamster ovary (CHO) cells with FSHR gene promoter constructs, cells (60% to 70% confluent) were preincubated in OptiMEM medium (Lipofectamine, Gibco BRL) for 30 minutes at 37°C. FSHR gene promoter plasmids (1 μg) and a plasmid containing TK-driven pRL (Toyo Ink, 200 ng, used to normalize for transfection efficiency) were mixed with liposome suspension (Lipofectamine,

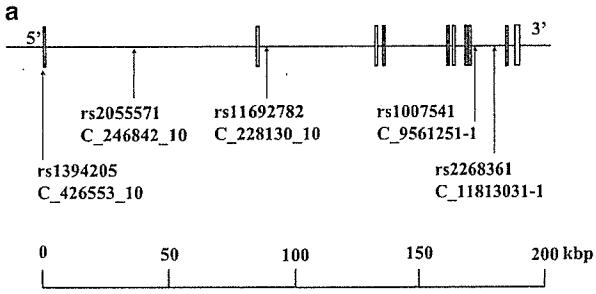

b

SNP	rs1394205	rs2055571	rs11692782	rs1007541	rs2268361
rs1394205	|D'|	0.969	0.011	0.297	0.064
	r^2	0.355	0.000	0.051	0.003
	rs2055571	|D'|	0.785	0.025	0.299
		r^2	0.199	0.000	0.452
		rs11692782	|D'|	0.498	0.298
			r^2	0.132	0.057
			rs1007541	|D'|	0.455
				r^2	0.173

|D'|>0.50

R^2<0.1

c

-150 CTAATGGTTATATTTGCTGTGTGCCTTAGGTCAGGGTGTAAGAAACCCAA

-100 TCTTGAAGGAAAACAGAGTAGCTTATCTTGCCTGGAAGTAACAAAAAAAA

-50 AAAAAAAAAGCATCCCTTGGTGGGTCACATGACCCTACCAGTTCTCAAGT

+1 CAGATCTCTTCTCATAAGGGCACTGTGTGGAGCTTCTGAGATCTGTGGAG

+50 GTTTTTCTCTGCAAATGCAGGAAGAAATCAGGTGGATGGATGCATAATTA

TGGCC A

Figure 1. a, Organization of the human FSH receptor gene and location of the SNPs used for the present case–control study. ■, exons, and —, indicate introns. b, Pairwise LD in the FSH receptor gene, as evaluated by D′ and r^2. Pairwise LD among the 6 marker pairs studied in the FSH receptor gene were computed, and pairs in LD (D′>0.5 or r^2<0.1) are shown as gray-shaded values. c, Nucleotide sequence of the 5′ upstream region of the FSH receptor gene. →, the major transcriptional initiation site, and the first nucleotide upstream of the transcriptional initiation site is designated −1. The G/A in bold type indicates the SNP of rs1394205. The italicized ATG indicates the start codon. Underlined nucleotide sequences indicate the PCR primers for making the insert of the plasmid that was used to measure transcriptional activities. The double underline indicates the *cis* element of the transcription factor Ets-1.

Gibco BRL, 6 μl/well) and incubated for 20 minutes at room temperature. The lipid-coated DNA was then added to each well containing 0.8 mL of OptiMEM media. After 3 hours, the medium was removed and replaced with complete medium for an additional 48 hours. CHO cells were then lysed (400 μL), and extracts were centrifuged to remove intact cells and debris. Extracts (50 μL) were used for measurement of luciferase activity. Luciferase activity was measured ≥3 times in duplicate with a double luciferase assay system (PicaGene Dual Sea-Pansy, Toyo Ink,) and a luminometer (LB-9507, Berthold). All of the data were normalized as relative light units/pRL-TK activity.[17]

Serum Levels of Estradiol

We measured serum levels of estradiol in female EH patients. Seventeen subjects in the female EH group were selected randomly. All of the subjects were confirmed to be postmenopausal by their own testimony. Six patients had the A/A genotype, and 12 patients had the G/A or G/G genotypes. Serum estradiol levels were measured with the Electro Chemil Luminescence Immunoassay (Elecsys Systems Immunoassay, Roche Diagnostics), as reported previously.[18]

Statistical Analysis

Data are shown as mean±SD. All of the statistical analyses were conducted using StatView 5.0 (SAS Inc) and Dr. SPSS II (SPSS Inc). Hardy–Weinberg equilibrium was assessed by a χ^2 analysis. The overall distributions of the genotypes or alleles were analyzed by χ^2 analysis using 2×3 or 2×2 contingency tables between EH patients and NT controls. To assess the quantitative effects of covariates, multiple logistic regression analysis was performed using SPSS II. Statistical significance was established at P<0.05.

Results

First Case–Control Study

Table 1 shows the distribution of genotypic and allelic frequencies of the 5 SNPs in each group. The observed and expected genotypic frequencies of each of the SNPs in the total subjects, male and female, of the NT group were in good agreement with the predicted Hardy–Weinberg equilibrium values (data not shown). The overall distribution of genotype and allele of all 5 of the SNPs did not significantly differ between men for the EH and NT groups. However, among women, the genotypic and allelic frequency of rs1394205 and the allelic frequency of rs2055571 showed a significant difference between the 2 groups. For the total subjects (male and female) the genotypic and allelic frequency of rs1394205 and the genotypic frequency of rs2268361 were significantly different between the EH and NT subjects. These data indicate that the distribution of rs1394205 in women can affect the overall analysis in the total subject group. Therefore, this could be used as a genetic marker of EH in women, because the probability value for the allelic distribution of this SNP was very significant (P=0.003).

Patterns of LD in the FSHR gene are illustrated by their D′ and r^2 values (Figure 1b). LD analysis for the NT group and the D′ values indicate that rs1394205 and rs2055571 are located in one haplotype block, whereas the other 3 SNPs are located in another block. Because the r^2 values were beyond 0.1 in rs1394205 to rs2055571, it is not advantageous to use these combinations to isolate susceptibility haplotypes.

Based on these results, rs1394205 was selected for the large-size case–control study. We were also interested in the fact that the rs1394205 may influence the transcriptional activity of the gene, because the SNP is located in the 5′ upstream region.

Confirmative Case–Control Study: Subgroup Collaboration Study With the Hypertensive Section of the Japanese Millennium Project

Table 2 shows the clinical features of the EH patients and NT controls. These 2 groups were age-matched for the total, male, and female groups. We performed the confirmative case–control study for the rs1394205 SNP using 1035 EH patients and 1058 NT controls.

TABLE 1. Genotype Distribution in NTs and Patients With EH of First Screening Analysis

	Total Subjects			Male Subjects			Female Subjects		
Parameters	NT	EH	*P*	NT	EH	*P*	NT	EH	*P*
No. of participants	235	237		152	158		83	79	
Variants									
rs1394205									
Genotype									
GG	64 (0.272)	45 (0.190)		34 (0.224)	30 (0.190)		30 (0.361)	15 (0.190)	
GA	123 (0.524)	125 (0.527)		81 (0.533)	84 (0.532)		42 (0.506)	41 (0.519)	
AA	48 (0.204)	67 (0.283)	0.040*	37 (0.243)	44 (0.278)	0.673	11 (0.133)	23 (0.291)	0.010*
Allele									
G	251 (0.534)	215 (0.454)		149 (0.490)	144 (0.456)		102 (0.614)	71 (0.449)	
A	219 (0.466)	259 (0.546)	0.013*	155 (0.510)	172 (0.544)	0.391	64 (0.386)	87 (0.551)	0.003*
rs2055571									
Genotype									
TT	121 (0.515)	140 (0.591)		82 (0.540)	93 (0.589)		39 (0.470)	47 (0.594)	
TC	93 (0.396)	84 (0.354)		59 (0.388)	55 (0.348)		34 (0.410)	29 (0.367)	
CC	21 (0.089)	13 (0.055)	0.156	11 (0.072)	10 (0.063)	0.683	10 (0.120)	3 (0.038)	0.090
Allele									
T	335 (0.713)	364 (0.768)		223 (0.734)	241 (0.763)		112 (0.675)	123 (0.778)	
C	135 (0.287)	110 (0.232)	0.053	81 (0.266)	75 (0.237)	0.404	54 (0.325)	35 (0.222)	0.036*
rs11692782									
Genotype									
AA	54 (0.23)	63 (0.266)		33 (0.217)	39 (0.247)		21 (0.253)	24 (0.304)	
AT	121 (0.515)	108 (0.456)		77 (0.507)	74 (0.468)		44 (0.530)	34 (0.430)	
TT	60 (0.255)	66 (0.278)	0.426	42 (0.276)	45 (0.285)	0.761	18 (0.217)	21 (0.266)	0.446
Allele									
A	229 (0.487)	234 (0.494)		143 (0.470)	152 (0.481)		86 (0.518)	82 (0.519)	
T	241 (0.513)	240 (0.506)	0.843	161 (0.530)	164 (0.519)	0.791	80 (0.482)	76 (0.481)	0.987
rs1007541									
Genotype									
GG	100 (0.426)	80 (0.338)		59 (0.388)	53 (0.335)		41 (0.494)	27 (0.342)	
GA	104 (0.442)	122 (0.514)		72 (0.474)	84 (0.532)		32 (0.386)	38 (0.481)	
AA	31 (0.132)	35 (0.148)	0.143	21 (0.138)	21 (0.133)	0.569	10 (0.120)	14 (0.177)	0.138
Allele									
G	304 (0.647)	282 (0.595)		190 (0.625)	190 (0.601)		114 (0.687)	92 (0.582)	
A	166 (0.353)	192 (0.405)	0.101	114 (0.375)	126 (0.399)	0.544	52 (0.313)	66 (0.418)	0.051
rs2268361									
Genotype									
GG	48 (0.204)	53 (0.224)		30 (0.197)	34 (0.215)		18 (0.217)	19 (0.241)	
GA	102 (0.434)	123 (0.519)		67 (0.441)	82 (0.519)		35 (0.422)	41 (0.518)	
AA	85 (0.362)	61 (0.257)	0.046*	55 (0.362)	42 (0.266)	0.184	30 (0.361)	19 (0.241)	0.238
Allele									
G	198 (0.421)	229 (0.483)		127 (0.418)	150 (0.475)		71 (0.428)	79 (0.500)	
A	272 (0.579)	245 (0.517)	0.056	177 (0.582)	166 (0.525)	0.154	95 (0.572)	79 (0.500)	0.192

*Significant difference in distribution.

The observed and expected genotypic frequencies of each of the SNPs in the total subjects (P=0.553), males (P=0.853), and females (P=0.426) of the NT group were in good agreement with the predicted Hardy–Weinberg equilibrium values. The overall distribution for the alleles of the SNPs did not significantly differ between the total EH and total NT groups. However, among women, the allelic frequency of the A allele of rs1394205 was significantly higher for EH subjects than for NT subjects (P=0.042; Table 3). Although the genotype distribution of rs1394205 among women in the first case–control study showed

TABLE 2. Characteristics of Study Participants of Subgroup Analysis of the Hypertension Team in Japanese Millennium Project

	Total			Male			Female		
Parameters	NT	EH	*P*	NT	EH	*P*	NT	EH	*P*
No. of subjects	1058	1035		792	762		266	273	
Age, y	60.4±7.9	59.7±9.5	0.052	59.6±7.3	59.1±8.7	0.269	63.0±9.1	61.3±11.1	0.051
BMI, kg/m^2	22.4±2.7	23.5±2.8	<0.001*	22.5±2.8	23.4±2.5	<0.001*	22.2±2.7	23.8±3.6	<0.001*
SBP, mm Hg	114.1±10.2	161.5±22.3	<0.001*	114.6±10.4	160.8±21.3	<0.001*	111.4±8.6	164.0±25.2	<0.001*
DBP, mm Hg	70.2±7.0	97.1±14.4	<0.001*	70.6±6.9	97.2±14.0	<0.001*	68.1±7.2	96.8±15.9	<0.001*
Total cholesterol, mg/dL	203.3±36.0	204.2±34.0	0.609	198.4±34.3	198.8±32.2	0.818	215.7±37.1	218.5±34.7	0.364
Triglyceride, mg/dL	116.5±74.2	143.7±97.9	<0.001*	117.4±7.6	146.3±102.2	<0.001*	114.3±67.7	135.2±72.7	0.002*
HDL cholesterol, mg/dL	56.8±14.8	58.4±16.5	0.043*	55.7±14.6	57.7±16.4	0.022*	59.5±15.0	60.0±16.6	0.736
Uric acid, mg/dL	5.3±2.6	5.7±2.4	0.004*	5.6±1.3	6.1±2.7	<0.001*	4.8±4.3	4.8±1.1	0.962
Creatinine, mg/dL	0.81±0.19	0.83±0.27	0.106	0.86±0.18	0.89±0.29	0.015*	0.71±0.17	0.69±0.17	0.372
γ -GTP	35.4±39.7	52.0±71.7	<0.001*	44.4±46.5	68.1±87.1	<0.001*	25.8±27.9	29.5±29.8	0.190
Smoking, %	45	46.6	0.583	66.6	62.1	0.182	4.6	7.3	0.271
Alcohol consumption, %	49.1	43.2	0.045*	62.9	74.3	0.001*	25.2	17.1	0.053

BMI indicates body mass index.
*Significant difference in distribution.

a significant difference, the genotype distribution in the confirmative study did not exhibit any significant difference. This discrepancy could have been caused by differences in sample size.

Multiple logistic regression analysis in the female subjects revealed that the significant association of A/A and G/A with EH (P=0.033) remained after adjustment for confounding factors (such as age, body mass index, total cholesterol, triglyceride, high-density lipoprotein cholesterol, uric acid, and creatinine), and the calculated odds ratio was 1.68 (95% CI: 1.04 to 2.73).

Transcriptional Activities

To study transcriptional activity, we transfected CHO cells with promoter constructs of the FSHR gene. The promoter activity of the A allele was 56±8% (mean±SD) of that for the G-type allele (P=0.001; Figure 2). The rs1394205 is located in the Ets-1 site, and when there is substitution of the A-type allele from the G-type allele, the Ets-1 site vanishes (Figure 1c).

Serum Levels of Estradiol

All of the values of the serum levels of estradiol were <32 pg/mL, because all of the subjects were postmenopausal. The values of G/G, G/A, and A/A genotypes were 19.8±2.1, 20.5±6.2, and 13.3±3.2, respectively. Because there was no difference between the G/G and G/A genotypes (P=0.807), Figure 3 only shows the serum levels of estradiol in postmenopausal EH patients with and without the A/A genotype. Serum estradiol levels were significantly lower in patients with the A/A genotype than in patients without the A/A genotype (P=0.004).

Discussion

We performed 2 genetic case–control studies in different populations for the FSHR gene and found that the SNP in the

TABLE 3. Genotype Distribution in NTs and Patients With Essential Hypertension of Subgroup Analysis of Hypertension in Japanese Millennium Project

	Total Subjects			Male			Female		
Parameters	NT	EH	*P*	NT	EH	*P*	NT	EH	*P*
No. of participants	1058	1035		792	762		266	273	
Variants									
rs1394205									
Genotype									
GG	297 (0.281)	253 (0.244)		212 (0.268)	184 (0.242)		85 (0.320)	69 (0.253)	
GA	518 (0.489)	531 (0.513)		393 (0.496)	400 (0.525)		125 (0.470)	131 (0.480)	
AA	243 (0.230)	251 (0.243)	0.169	187 (0.236)	178 (0.233)	0.431	56 (0.210)	73 (0.267)	0.139
Allele									
G	1112 (0.526)	1037 (0.501)		817 (0.516)	768 (0.504)		295 (0.555)	269 (0.493)	
A	1004 (0.474)	1033 (0.499)	0.112	767 (0.484)	756 (0.496)	0.509	237 (0.445)	277 (0.507)	0.04*

*Significant difference in distribution.

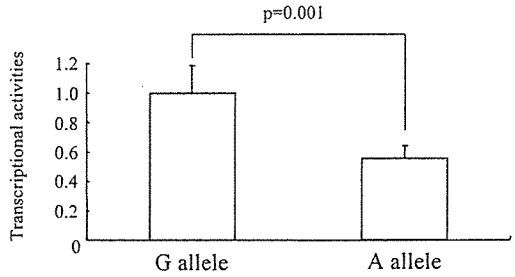

Figure 2. Transcriptional activities of the reporter constructs. The activities of the G-type constructs were considered as 100%. Values are expressed as the average of 3 independent experiments done on different days. Data are mean±SD.

5′-untranslated region of the FSHR gene affects levels of transcriptional activity and is a susceptibility mutation of EH in women. Very recently it has been reported that knockout mice can be used as a model of postmenopausal hypertension with low levels of estrogen and high levels of testosterone.[14] This report is consistent with our results that indicate that there is both an association between the polymorphism in the FSHR gene and EH and that the levels of plasma estradiol in female EH patients with the A/A genotype are significantly lower than those in female EH patients without the genotype. Furthermore, because Ets-1 has been reported to be involved in the regulation of angiogenesis and cell growth,[19,20] our findings suggest that the substitution of the A-type allele from the G-type allele of the rs1394205 leads to a decreased transcriptional activity, which is followed by a subsequent loss of the Ets-1 site. Because there have been many studies reporting that low estrogen levels are associated with hypertension in postmenopausal women,[21,22] our results also may provide evidence on the etiology of ≥1 of the causes of hypertension in postmenopausal women.

In genetic case–control studies, pseudopositive results can sometimes occur. Therefore, to improve reliability, we increased the number of samples in addition to selecting samples strictly for the purpose of removing bias associated with confounding factors. It is especially advantageous to perform case–control studies using large and different populations, because this can lead to results that have a greater likelihood of being correct. The strategy of our study was to first carry out a screening case–control study followed by a confirmative case–control study that included >1000 subjects in each group. The rs1394205 showed significant differences for both case–control studies. It should be noted that the *P* values for the associations determined in the present study are somewhat weak. However, in accordance with the guidelines issued for specific criteria for acceptability of association study results, the current study provides biological support (transient transfection finding) and plausibility based on knockout data in mice.[23] Therefore, the larger *P* value could be considered to be acceptable in this case.

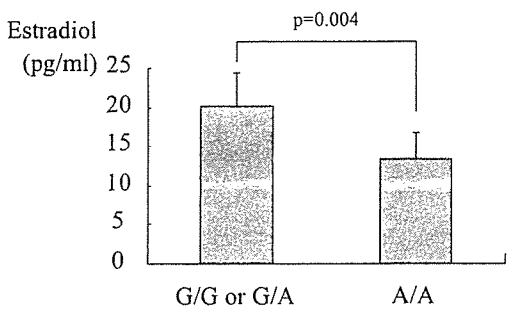

Figure 3. Serum levels of estradiol. Data are mean±SD.

Some case–control studies have identified gene variants associated with gender-specific susceptibility to EH[24,25]; however, in general, such studies do not explain the reason for the positive gender-specific association findings. Our experiment also found significant differences only for women. In contrast to previous reports, our experiment specifically examined whether the functional mutations of the gene were clearly identified in patients with a hereditary disease in a gender-specific manner. Mutations in the FSHR gene are reported to cause hereditary hypergonadotropic ovarian failure in women but not in men. To the best of our knowledge, our study is the first to report that the causal genes of gender-specific hereditary diseases are associated with EH in a gender-specific manner.

An increasing number of reports of genome-wide scans for hypertension and blood pressure variation have been seen in the past few years.[26] Some of the reports have shown that 2p, on which the FSHR gene is located, is associated with the candidate loci for EH.[27–32] However, these regions are broad, and there has been no definite susceptibility gene identified in this region. Although like our study in which the strategy for identification of susceptibility genes of EH was different between the genome-wide scans and case–control studies, the final goal for identifying the causal mutation for EH was the same. Therefore, because our current findings indicate that a gene variant is related to EH, our results are thought to be worthwhile. In conclusion, an SNP in the 5′-untranslated region of the FSHR gene affected the levels of transcriptional activity and, therefore, is a susceptibility mutation of EH in women.

Perspectives

We performed 2-step case–control studies and identified that the SNP in the 5′-untranslated region of the FSHR gene affects levels of transcriptional activity, which is a susceptibility mutation of EH in women. However, there are some limitations associated with our study. It is possible that the case–control studies sometimes exhibit pseudopositive results because of sample scales or selection of the genetic markers. Further research is required to perform familial linkage studies and transmission disequilibrium tests for the purpose of confirming the reliability of the rs1394205 SNP.

Acknowledgments

We thank Naoyuki Sato and Kaoru Sugama for their excellent technical assistance.

Sources of Funding

This work was supported in part by a Grant-in-Aid for Scientific Research on Priority Areas (15012251) from the Ministry of Education, Culture, Sports, Science and Technology.

Disclosures

None.

References

1. Dominiczak AF, Negrin DC, Clark JS, Brosnan MJ, McBride MW, Alexander MY. Genes and hypertension: from gene mapping in experimental models to vascular gene transfer strategies. *Hypertension*. 2000; 35:164–172.
2. Colhoun H. Confirmation needed for genes for hypertension. *Lancet*. 1999;353:1200–1201.
3. Johnson GL, Dhanasekaran N. The G-protein family and their interaction with receptors. *Endocr Rev*. 1989;10:317–331.
4. McFarland KC, Sprengel R, Phillips HS, Kohler M, Rosemblit N, Nikolics K, Segaloff DL, Seeburg PH. Lutropin-choriogonadotropin receptor: an unusual member of the G protein-coupled receptor family. *Science*. 1989;245:494–499.
5. Parmentier M, Libert F, Maenhaut C, Lefort A, Gerard C, Perret J, Van Sande J, Dumont JE, Vassart G. Molecular cloning of the thyrotropin receptor. *Science*. 1989;246:1620–1622.
6. Sprengel R, Braun T, Nikolics K, Segaloff DL, Seeburg PH. The testicular receptor for follicle stimulating hormone: structure and functional expression of cloned cDNA. *Mol Endocrinol*. 1990;4:525–530.
7. Minegishi T, Nakamura K, Takakura Y, Ibuki Y, Igarashi M. Cloning and sequencing of human FSH receptor cDNA. *Biochem Biophys Res Commun*. 1991;175:1125–1130.
8. Gromoll J, Dankbar B, Gudermann T. Characterization of the 5′ flanking region of the human follicle-stimulating hormone receptor gene. *Mol Cell Endocrinol*. 1994;102:93–102.
9. Aittomaki K, Lucena JL, Pakarinen P, Sistonen P, Tapanainen J, Gromoll J, Kaskikari R, Sankila EM, Lehvaslaiho H, Engel AR, Nieschlag E, Huhtaniemi I, de la Chapelle A. Mutation in the follicle-stimulating hormone receptor gene causes hereditary hypergonadotropic ovarian failure. *Cell*. 1995;82:959–968.
10. Tapanainen JS, Aittomaki K, Min J, Vaskivuo T, Huhtaniemi IT. Men homozygous for an inactivating mutation of the follicle-stimulating hormone (FSH) receptor gene present variable suppression of spermatogenesis and fertility. *Nat Genet*. 1997;15:205–206.
11. Dierich A, Sairam MR, Monaco L, Fimia GM, Gansmuller A, LeMeur M, Sassone-Corsi P. Impairing follicle-stimulating hormone (FSH) signaling in vivo: Targeted disruption of the FSH receptor leads to aberrant gametogenesis and hormonal imbalance. *Proc Natl Acad Sci U S A*. 1998;95: 13612–13617.
12. Danilovich N, Harada N, Sairam MR, Maysinger D. Age-related neurodegenerative changes in the central nervous system of estrogen-deficient follitropin receptor knockout mice. *Exp Neurol*. 2003;183:559–572.
13. Grover A, Sairam MR, Smith CE, Hermo L. Structural and functional modifications of sertoli cells in the testis of adult follicle-stimulating hormone receptor knockout mice. *Biol Reprod*. 2004;71:117–129.
14. Javeshghani D, Touyz RM, Sairam MR, Virdis A, Neves MF, Schiffrin EL. Attenuated responses to angiotensin II in follitropin receptor knockout mice, a model of menopause-associated hypertension. *Hypertension*. 2003;42:761–767.
15. Nakayama T, Soma M, Sato N, Haketa A, Kosuge K, Aoi N, Sato M, Izumi Y, Matsumoto K, Kanmatsuse K, Kokubun S. An association study in essential hypertension using functional polymorphisms in lymphotoxin-α gene. *Am J Hypertens*. 2004;17:1045–1049.
16. Sano M, Kuroi N, Nakayama T, Sato N, Izumi Y, Soma M, Kokubun S. The association study of calcitonin-receptor-like receptor gene in essential hypertension. *Am J Hypertens*. 2005;18:403–408.
17. Nakayama T, Soma M, Takahashi Y, Rehemudula D, Kanmatsuse K, Furuya K. Functional deletion mutation of the 5′-flanking region of the type A human natriuretic peptide receptor gene and its association with essential hypertension and left ventricular hypertrophy in the Japanese. *Circ Res*. 2000;86:841–845.
18. Saavedra I, Leon J, Prado J, Sanchez MP, Lopez F, Gaete L. A comparative pharmacokinetic study of micronized estradiol valerate administered alone and in combination with medroxyprogesterone acetate in postmenopausal women. *Ther Drug Monit*. 2004;26:482–485.
19. Hashiya N, Jo N, Aoki M, Matsumoto K, Nakamura T, Sato Y, Ogata N, Ogihara T, Kaneda Y, Morishita R. In vivo evidence of angiogenesis induced by transcription factor Ets-1: Ets-1 is located upstream of angiogenesis cascade. *Circulation*. 2004;109:3035–3041.
20. Sakaguchi H, Fujimoto J, Aoki I, Toyoki H, Sato E, Tamaya T. Expression of E26 transformation specific (ETS-1) related to angiogenesis in ovarian endometriosis. *Fertil Steril*. 2004;82:507–510.
21. Aldrighi JM, Alecrin IN, Caldas MA, Gebara OC, Ramires JA, Rosano GM. Effects of estradiol on myocardial global performance index in hypertensive postmenopausal women. *Gynecol Endocrinol*. 2004;19: 282–292.
22. Fak AS, Erenus M, Tezcan H, Caymaz O, Oktay S, Oktay A. Effects of a single dose of oral estrogen on left ventricular diastolic function in hypertensive postmenopausal women with diastolic dysfunction. *Fertil Steril*. 2000;73:66–71.
23. Freimer NB, Sabatti C. Guidelines for association studies in Human Molecular Genetics. *Hum Mol Genet*. 2005;14:2481–2483.
24. O'Donnell CJ, Lindpaintner K, Larson MG, Rao VS, Ordovas JM, Schaefer EJ, Myers RH, Levy D. Evidence for association and genetic linkage of the angiotensin-converting enzyme locus with hypertension and blood pressure in men but not women in the Framingham Heart Study. *Circulation*. 1998;97:1766–1772.
25. Ono K, Mannami T, Iwai N. Association of a promoter variant of the haeme oxygenase-1 gene with hypertension in women. *J Hypertens*. 2003;21:1497–1503.
26. Mein CA, Caulfield MJ, Munroe PB. Selection of candidate genes in hypertension. *Methods Mol Med*. 2005;108:107–129.
27. Krushkal J, Ferrell R, Mockrin SC, Turner ST, Sing CF, Boerwinkle E. Genome-wide linkage analyses of systolic blood pressure using highly discordant siblings. *Circulation*. 1999;99:1407–1410.
28. Rice T, Rankinen T, Province MA, Chagnon YC, Perusse L, Borecki IB, Bouchard C, Rao DC. Genome-wide linkage analysis of systolic and diastolic blood pressure: the Quebec Family Study. *Circulation*. 2000; 102:1956–1963.
29. Atwood LD, Samollow PB, Hixson JE, Stern MP, MacCluer JW. Genome-wide linkage analysis of blood pressure in Mexican Americans. *Genet Epidemiol*. 2001;20:373–382.
30. Rice T, Rankinen T, Chagnon YC, Province MA, Perusse L, Leon AS, Skinner JS, Wilmore JH, Bouchard C, Rao DC. Genomewide linkage scan of resting blood pressure: HERITAGE Family Study. Health, risk factors, exercise training, and genetics. *Hypertension*. 2002;39:1037–1043.
31. Angius A, Petretto E, Maestrale GB, Forabosco P, Casu G, Piras D, Fanciulli M, Falchi M, Melis PM, Palermo M, Pirastu M. A new essential hypertension susceptibility locus on chromosome 2p24–p25, detected by genomewide search. *Am J Hum Genet*. 2002;71:893–905.
32. Rao DC, Province MA, Leppert MF, Oberman A, Heiss G, Ellison RC, Arnett DK, Eckfeldt JH, Schwander K, Mockrin SC, Hunt SC; HyperGEN Network. A genome-wide affected sibpair linkage analysis of hypertension: the HyperGEN network. *Am J Hypertens*. 2003;16: 148–150.

Haplotypes of the plasminogen activator gene associated with ischemic stroke

Kosuke Saito[1,2], Tomohiro Nakayama[1], Naoyuki Sato[1], Akihiko Morita[3], Teruyuki Takahashi[4], Masayoshi Soma[5], Ron Usami[2]

[1]Division of Molecular Diagnostics, Advanced Medical Research Center, Nihon University School of Medicine, Tokyo, Japan; [2]Department of Biological Applied Chemistry, Toyo University Graduate School of Engineering, Saitama, Japan; [3]Department of Neurology, Division of Neurology, Department of Medicine, Nihon University School of Medicine, Tokyo, Japan; [4]Department of Neurology, Graduate School of Medicine, Nihon University, Tokyo, Japan; [5]Division of Nephrology and Endocrinology, Department of Medicine, Nihon University School of Medicine, Tokyo, Japan

Summary

Ischemic stroke (IS) is thought to be a multifactorial disorder associated with genetic backgrounds and environmental factors. In the circulating plasma, tissue plasminogen activator (tPA) catalyzes the reaction from plasminogen to plasmin. If there is a functional disability of tPA, induction of thrombosis and infarction disorders can occur. The aim of this study was to perform a haplotype-based case-control study using single nucleotide polymorphisms (SNPs) in the human tPA gene, and to assess the association between the tPA gene and IS. We genotyped 182 IS individuals and 403 controls for five SNPs in the human tPA gene, rs7007329, rs732612, rs8178750, rs2020922, and rs4471024. Using these five SNPs, a haplotype-based case control study was performed. There were seven SNP combinations that exhibited significant differences in the overall distribution between the IS and control groups. Linkage disequilibrium analysis showed that the combination of rs7007329 and rs8178750 was useful in identification of the susceptibility haplotype. The frequency of the G-T haplotype at rs7007329-rs8178750 was significantly higher in the IS group (1.2%) as compared to the control group (0.0%) (p=0.003). Diplotype analysis also showed a significant association of the diplotype with the G-T haplotype at rs7007329-rs8178750 (OR:11.4, 95%CI:1.32–97.9, p=0.013). These results suggest that the G-T haplotype at rs7007329-rs8178750 of the tPA gene is a genetic marker for IS, and that tPA or a neighboring gene is a susceptibility gene for IS.

Keywords

Tissue plasminogen activator, ischemic stroke, haplotypes, association studies, genetics

Thromb Haemost 2006; 96: 331–6

Introduction

Ischemic stroke (IS) is thought to be a multifactorial disorder caused by interaction between various genetic factors and several environmental factors. Together, the different environmental and genetic factors lead to development of IS (1). The different susceptibility polymorphisms and mutations exert their effects in a polygenic context. Identifying genetic factors as susceptibility genes is very important for polygenic disorders. At the present time, certain susceptibility genes have yet to be identified.

Tissue plasminogen activator (tPA) catalyzes the conversion of zymogen plasminogen to the active enzyme plasmin in the fibrinolytic system. Plasmin dissolves the fibrin that is produced by the coagulation system. It has been reported that there is an association between coagulation factor gene and IS (2), and that high concentrations of tPA antigen could be a risk for development of stroke in healthy humans (3, 4). Several studies have shown that there is a relationship between the tPA antigen and cardiovascular events (5–7). Therefore, the human tPA gene is considered to be a susceptibility gene for the risk of IS.

The human tPA gene has been mapped to 8p12. It is composed of 14 exons and spans 32 kilobase pairs (kbp) (8). Recently, there have been reports on association studies using tPA gene polymorphism. Jannes et al. conjectured that the TT geno-

Correspondence to:
Tomohiro Nakayama, MD
Division of Molecular Diagnostics
Advanced Medical Research Center
Nihon University School of Medicine
Ooyaguchi-kamimachi, 30–1 Itabashi-ku
Tokyo 173–8610, Japan
Tel.: +81 3 3972 8111 ext. 2751, Fax: +81 3 5375 8076
E-mail: tnakayam@med.nihon-u.ac.jp

Received December 30, 2005
Accepted after resubmission July 28, 2006

Prepublished online August 16, 2006 doi:10.1160/TH05-12-0830

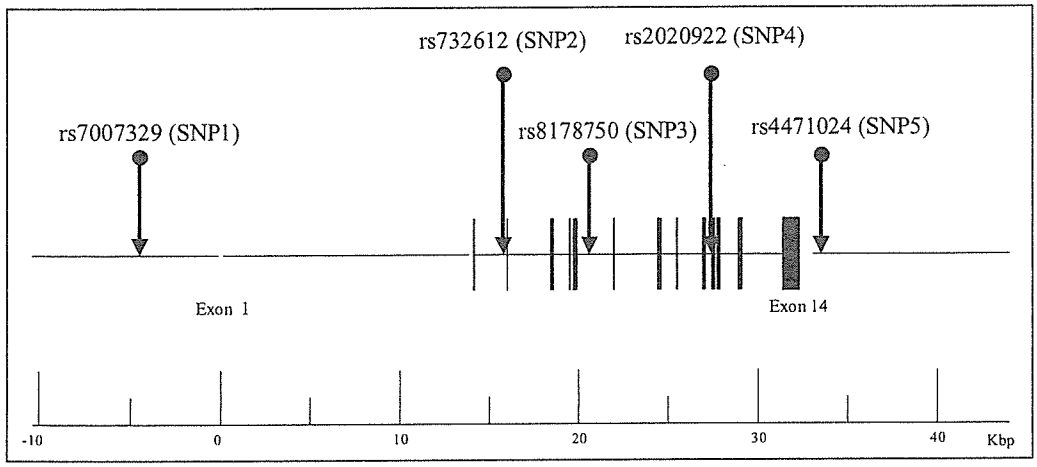

Figure 1: Organization of the human tPA gene and location of SNPs in the haplotype-based case-control study. Closed black boxes indicate coding exons and gray boxes indicate untranslated regions, and lines indicate introns.

type of the –7351C/T polymorphism located in the enhancer element of the tPA gene was involved in IS (9). However, their report did not examine the possibility of an association between other polymorphisms and the tPA gene.

The aim of the present study was to perform a haplotype-based case-control study using single nucleotide polymorphisms (SNPs) in the human tPA gene in order to assess the association between the tPA gene and IS in Japanese subjects.

Materials and methods

Study population

Patients and control subjects from the northern area of Tokyo were recruited for the case-control study. Patients were selected and consecutively recruited from among those who were admitted at our hospital (Nihon University Hospital in Tokyo) or community hospital in Tokyo between 1995 and 2005. Control subjects were selected from among subjects that were outpatients at our hospital during the same period. Our experiment was not a population-based study, as more than 80% of the approximately 500 subjects we approached agreed to participate in the study. We applied strict criteria regarding the selection of subjects for participation in this case-control study (10).

The study group consisted of 182 Japanese patients (mean age, 65.2 ± 12.3 years) with IS that had been diagnosed either by computed tomography (CT) or magnetic resonance imaging (MRI). All patients had neurological deficits that persisted for three months. For controls, a total of 403 Japanese control subjects (mean age, 63.5 ± 15.1 years) were studied. We selected the control subjects having vascular risk factors such as hypertension, hypercholesterolemia, or diabetes mellitus, but no ischemic cerebrovascular disease, because not matched parameters between the patients and controls sometimes induced results of bias. Patients with anti-phospholipid antibody syndrome and atrial fibrillation were excluded from the study group. Histories of alcohol and tobacco use were also recorded. Habitual drinkers

Table 1: Characteristics of study participants.

	Total		P-value	Men		P-value	Women		P-value
	IS	Control		IS	Control		IS	Control	
Number of subjects	182	403		108	234		74	169	
Age (years)	65.2 ± 12.3	63.5 ± 15.1	0.166	63.3 ± 11.4	62.3 ± 14.7	0.546	68.1 ± 13.0	65.1 ± 15.4	0.143
BMI (mg/m^2)	23.4 ± 3.5	22.7 ± 3.0	0.020	23.2 ± 2.9	22.9 ± 3.1	0.346	23.9 ± 4.6	22.4 ± 2.9	0.013
SBP (mmHg)	152.9 ± 27.0	123.2 ± 17.8	<0.001	151.4 ± 26.5	122.2 ± 16.7	<0.001	155.0 ± 27.8	124.7 ± 19.1	<0.001
DBP (mmHg)	86.6 ± 16.1	73.5 ± 10.7	<0.001	87.6 ± 16.3	73.4 ± 10.2	<0.001	85.0 ± 15.8	73.6 ± 11.4	<0.001
Pulse (beats/min)	76.6 ± 14.5	71.1 ± 10.8	<0.001	75.8 ± 14.3	70.1 ± 10.8	<0.001	77.7 ± 14.7	72.5 ± 10.7	0.004
Creatinine (mg/dl)	1.14 ± 1.20	0.85 ± 0.48	<0.001	1.25 ± 1.21	0.94 ± 0.59	0.002	0.99 ± 1.18	0.72 ± 0.18	0.004
Total cholesterol (mg/dl)	201.6 ± 51.0	210.1 ± 45.1	0.048	196.6 ± 50.3	201.6 ± 36.1	0.309	208.7 ± 51.3	222.0 ± 53.1	0.079
HDL cholesterol (mg/dl)	50.0 ± 20.3	57.0 ± 17.2	0.001	47.1 ± 20.2	55.2 ± 16.4	0.001	54.6 ± 19.6	60.7 ± 18.5	0.083
Uric acid (mg/dl)	5.6 ± 2.3	5.3 ± 1.4	0.080	5.9 ± 2.0	5.7 ± 1.3	0.379	5.2 ± 2.6	4.5 ± 1.2	0.026
Alcohol consumption (%)	47.1	53.1	0.279	67.1	65.3	0.782	17.5	31.6	0.024
Smoking (%)	50.0	38.3	0.028	69.3	50.3	0.006	21.6	19.6	0.807

IS, ischemic stroke; control, non-ischemic stroke subjects; BMI, body mass index; SBP, systolic blood pressure; DBP, diastolic blood pressure; HDL, high density lipoprotein; Alcohol consumption (%) and Smoking (%), the proportion of subjects that had histories of alcohol use and smoking.

Table 2: Genotype distribution in control subjects and patients with IS.

		Total		P-value	Men		P-value	Women		P-value
		IS	Control		IS	Control		IS	Control	
Number of participants		182	403		108	234		74	169	
rs7007329	Genotype									
	GG	16 (0.088)	31 (0.077)		12 (0.111)	16 (0.068)		4 (0.054)	15 (0.089)	
	GC	64 (0.352)	169 (0.419)		35 (0.192)	93 (0.397)		29 (0.392)	76 (0.450)	
	CC	102 (0.560)	203 (0.504)	0.300	61 (0.335)	125 (0.534)	0.242	41 (0.554)	78 (0.461)	0.352
	Allele									
	G	96 (0.264)	231 (0.287)		59 (0.273)	125 (0.267)		37 (0.250)	106 (0.314)	
	C	268 (0.736)	575 (0.713)	0.420	157 (0.727)	343 (0.733)	0.868	111 (0.750)	232 (0.686)	0.157
rs732612	Genotype									
	CC	35 (0.192)	72 (0.179)		20 (0.185)	39 (0.167)		15 (0.203)	33 (0.195)	
	CA	91 (0.500)	203 (0.503)		56 (0.519)	124 (0.530)		35 (0.473)	79 (0.467)	
	AA	56 (0.308)	128 (0.318)	0.918	32 (0.296)	71 (0.303)	0.915	24 (0.324)	57 (0.337)	0.978
	Allele									
	C	161 (0.442)	347 (0.431)		96 (0.444)	202 (0.432)		65 (0.439)	145 (0.429)	
	A	203 (0.558)	459 (0.569)	0.707	120 (0.556)	266 (0.568)	0.753	83 (0.561)	193 (0.571)	0.835
rs8178750	Genotype									
	TT	2 (0.011)	2 (0.005)		1 (0.009)	0 (0.000)		1 (0.014)	2 (0.012)	
	TC	8 (0.044)	16 (0.040)		6 (0.056)	10 (0.043)		2 (0.027)	6 (0.036)	
	CC	172 (0.945)	385 (0.955)	0.692	101 (0.935)	224 (0.957)	—	71 (0.959)	161 (0.952)	0.939
	Allele									
	T	12 (0.033)	20 (0.025)		8 (0.037)	10 (0.021)		4 (0.027)	10 (0.030)	
	C	352 (0.967)	786 (0.975)	0.429	208 (0.963)	458 (0.979)	0.234	144 (0.973)	328 (0.970)	0.877
rs2020922	Genotype									
	TT	91 (0.500)	201 (0.499)		55 (0.509)	116 (0.496)		36 (0.486)	85 (0.503)	
	TA	73 (0.401)	164 (0.407)		39 (0.361)	95 (0.406)		34 (0.459)	69 (0.408)	
	AA	18 (0.099)	38 (0.094)	0.981	14 (0.130)	23 (0.098)	0.583	4 (0.055)	15 (0.089)	0.566
	Allele									
	T	255 (0.701)	566 (0.702)		149 (0.690)	327 (0.699)		106 (0.716)	239 (0.707)	
	A	109 (0.299)	240 (0.298)	0.954	67 (0.310)	141 (0.301)	0.814	42 (0.284)	99 (0.293)	0.839
rs4471024	Genotype									
	GG	35 (0.192)	72 (0.179)		20 (0.185)	39 (0.167)		15 (0.203)	33 (0.196)	
	GA	92 (0.505)	203 (0.503)		57 (0.528)	124 (0.530)		35 (0.473)	79 (0.467)	
	AA	55 (0.302)	128 (0.318)	0.894	31 (0.287)	71 (0.303)	0.899	24 (0.324)	57 (0.337)	0.978
	Allele									
	G	162 (0.445)	347 (0.431)		97 (0.449)	202 (0.432)		65 (0.439)	145 (0.429)	
	A	202 (0.555)	459 (0.569)	0.643	119 (0.551)	266 (0.568)	0.669	83 (0.561)	193 (0.571)	0.835

IS, ischemic stroke; controls, non-ischemic stroke subjects.

were defined as individuals who had ≥ 2–3 alcoholic beverages per day three times every week. Smokers were defined as current or former smokers, whereas non-smokers were defined as subjects with no history of previous or current smoking. Individuals who had stopped smoking <1 year prior to enrollment were classified as smokers.

To compare the results for the case-control study for IS, we attempted to perform another case-control study for essential hypertension (EH). EH subjects included 276 Japanese patients (mean age, 60.0 ± 5.6 years) with a diagnosis of EH according to the World Health Organization criteria (11), which required a sitting systolic blood pressure (SBP) of >160 mmHg and/or diastolic

blood pressure (DBP) of >100 mmHg on three different occasions during the two months following the first medical examination. None of the EH subjects were using antihypertensive medications. Patients diagnosed with secondary hypertension were excluded. The controls for this group included 283 Japanese normotensive (NT) healthy individuals (mean age, 77.9 ± 4.6 years). None of the control subjects had a family history of hypertension, and all had a SBP of <130 mmHg and a DBP of <85 mmHg. A family history of hypertension was defined as prior diagnosis of hypertension in a grandparent, uncle, aunt, parent or sibling. Both groups were recruited from the northern area of Tokyo, Japan.

Informed consent was obtained from each subject according to a protocol approved by the Human Studies Committee of Nihon University.

Biochemical analysis

Plasma concentrations of total and HDL-cholesterol and serum concentrations of creatinine and uric acid were measured using the methods of the Clinical Laboratory Department of Nihon University Hospital (12).

Genotyping

Based on information from the National Center for Biotechnology Information (NCBI) SNP database or the Applied Biosystems (Foster City, CA, USA) – Celera Discovery System (CDS) database (http://www.appliedbiosystems.com), we chose SNPs that had a minor allele frequency greater than 16%. We chose this frequency, as a previous report has shown that a SNP having a high minor allele frequency are useful in association studies using each SNP or haplotype (13). We selected five SNPs in the human tPA gene for the genetic association study between IS and control subjects (Fig. 1). rs7007329 (G/C) (SNP1) was located at –4360 nucleotides (nt) upstream of the transcription initiation site. rs732612 (C/A) (SNP2) was located at +15827 nt in intron 2. rs8178750 (T/C) (SNP3) was located at +20324 nt in intron 6. rs2020922 (T/A) (SNP4) was located at +27271 nt in intron 10. rs4471024 (G/A) (SNP5) was located at +624 nt downstream of the terminal codon. Genotypes were determined using Assays-on-Demand kits (Applied Biosystems) together with TaqMan® PCR, as has been previously described (14).

Haplotype-based case-control study and linkage disequilibrium and diplotype analysis

We performed the haplotype-based case-control study using 26 combinations established from the five SNPs. The frequency of each haplotype was estimated using the expectation/maximization (EM) algorithm (15, 16). In order to determine haplotype and linkage disequilibrium (LD), and for purposes of construction of the diplotype, SNPAlyze version 3.2 and version 3.2.3.pro were used (DYNACOM Co., Ltd. Yokohama, Japan). These are available from the developer's website (http://www.dynacom.co.jp/products/package/snpalyze/index.html).

Statistical analysis

Data are shown as mean ± SD. Differences in clinical data between the IS and control groups were assessed by analysis of variance (ANOVA) followed by a Fisher's protected least significant difference (PLSD) test.

Hardy-Weinberg equilibrium was assessed by a chi^2-analysis. When the sizes of the expected values were small (below 2.0), the genotypes with the small expected values were combined (17). The overall distribution of SNP alleles was analyzed by 2 x 2 contingency tables, and the distribution of the SNP genotypes between the IS patients and controls subjects was tested using a two-sided Fisher exact test (Dr. SPSS®; SPSS Japan Inc). Statistical significance was established at $p < 0.05$.

The threshold value of the frequencies of the haplotypes included in the analysis was set to 1%. All haplotypes below the threshold value were excluded from the analysis. Overall distribution of haplotypes was analyzed using 2 x m contingency tables with a value of $p < 0.05$ considered to indicate statistical significance. The p-value significance of each haplotype was determined by the chi^2-analysis and permutation method using the software SNPAlyze version 3.2 and 3.2.3 pro (14). Pair-wise linkage disequilibrium (LD) patterns for the tPA gene were evaluated using $|D'|$ and r^2 (18, 19). The criteria for $|D'|$ and r^2 values was set to $|D'| => 0.5$ and $r^2 => 0.25$.

Diplotype analyses were performed using two diplotype groups. In the first group there was more than one copy of the haplotype present while in the second group, there was either no

	(SNP1)	(SNP2)	(SNP3)	(SNP4)	SNP5)
SNPs	**rs7007329**	**rs732612**	**rs8178750**	**rs2020922**	**rs4471024**
rs7007329	|D'|	0.706	0.740	0.571	0.706
(SNP1)	r^2	0.265	0.006	0.308	0.265
	rs732612	|D'|	0.715	1.00	0.995
	(SNP2)	r^2	0.010	0.561	0.990
		rs8178750	|D'|	1.00	0.715
		(SNP3)	r^2	0.011	0.010
			rs2020922	|D'|	0.992
			(SNP4)	r^2	0.552
				rs4471024	|D'|
				(SNP5)	r^2

Table 3:
Pairwise linkage disequilibrium (LD) in the t-PA gene.
$|D'| => 0.5$ (dark grey),
$r^2 => 0.25$ (light grey)

Table 4: Haplotype distribution in the combination of SNP1-SNP3 for the two case-control study.

Combination of SNPs	Individual Haplotype	IS	Control	Chi^2	P-value	Permutation p-value
Rs7007329-rs8178750 (SNP1-SNP3)	C-C	0.715	0.692	0.616	0.433	0.431
	G-C	0.252	0.286	1.393	0.238	0.226
	C-T	0.021	0.022	0.002	0.965	0.892
	G-T	0.012	0.000	8.866	0.003*	0.014*
Combination of SNPs	**Individual Haplotype**	**EH**	**NT**	**Chi^2**	**P-value**	**Permutation p-value**
Rs7007329-rs8178750 (SNP1-SNP3)	C-C	0.709	0.716	0.068	0.794	0.796
	G-C	0.261	0.263	0.009	0.924	0.919
	C-T	0.021	0.018	0.223	0.637	0.633
	G-T	0.009	0.004	1.390	0.238	0.292

IS, ischemic stroke; control, non-ischemic stroke subjects; EH, essential hypertension; NT, normotension; *significant difference.

haplotype or different haplotypes present. A Fisher's exact test was performed for each of the diplotypes (Dr. SPSS®), and differences were considered statistically significant at $p<0.05$.

Results

Table 1 shows the characteristics of the study participants for patients with IS and for the control subjects. The systolic blood pressure (SBP), diastolic blood pressure (DBP), pulse, and creatinine levels were significantly higher between the two groups. No significant differences in age, uric acid, and alcohol consumption (%) were observed between the two groups.

Table 2 shows the genotype and allele distribution among patients in the IS and control groups. There were no significant differences for each of the SNPs.

We analyzed LD using the five SNPs in the control groups (Table 3). All |D'| values were more than 0.5, which indicates that all SNPs were located in one haplotype block. Furthermore, the high r^2 values of SNP1-SNP2, SNP1-SNP4, SNP1-SNP5, SNP2-SNP4, SNP2-SNP5, and SNP4-SNP5 were beyond 0.25, suggesting that SNP2 and SNP4 and SNP5 are not always necessary in order to perform a haplotype-based case-control study in this block. Therefore, we focused on the combination of SNP1-SNP3.

The results of the haplotype-based case-control study in all combinations for each of the SNPs are shown in Supplementary Table 1. There were seven of 26 combinations for which there were significant differences. Significant differences were also observed for the SNP1-SNP3 combination ($p=0.018$).

Individual haplotype distributions using the combination of SNP1-SNP3 in the two different case-control studies are presented in Table 4. There were no haplotypes that exhibited any significant differences in the EH-NT study, while the G-T haplotype at rs7007329-rs8178750 was significantly greater in the IS group (1.2%) as compared to the control group (0.0%) ($p=0.003$, permutation $p=0.014$).

Diplotype analysis showed a significant difference in distribution for the subjects with the G-T haplotype at rs7007329-rs8178750 between the IS and control groups (OR:11.4, 95%CI:1.32–97.9, $p=0.013$) (Table 5).

Discussion

In the present haplotype-based case-control study that used five SNPs, one haplotype (G-T of SNP1-SNP3) was observed to be associated with IS. Although the number of patients with the G-T haplotype at rs7007329-rs8178750 was small among the studied cases (1.2%), we believe that this finding is not insignificant. The results imply that IS pathogenesis is composed from the accumulation and interaction of multiple genetic loci, each of which have a weak phenotypic effect (20). Jood et al. reported that a genotype combination from the tPA –7351C/T polymorphism and plasminogen activator inhibitor type 1 (PAI-1) 675 4G/5G polymorphism were associated with a reduced risk of IS (21). Furthermore, the G-T haplotype at rs7007329-rs8178750 did not exhibit any significant difference in the other case-control study that examined EH patients. These results suggest that the G-T haplotype at rs7007329-rs8178750 is associated with IS as opposed to EH.

Although SNPs may be useful as genomic markers, they are not always useful in case-control studies, especially when using one SNP. However, haplotype-based case-control studies are thought to be more advantageous in the isolation of susceptibility genes and alleles. In genes with multiple susceptibility alleles, analyses based on haplotypes can have advantages over analyses based on individual SNPs, particularly when the LD between the SNPs is weak (22). These findings should encourage further development of statistical methods based on haplotypes that can be used to assess the potential of association methods in

Table 5: Diplotype analysis in the t-PA gene.

	IS	Control	OR	95% CI	P-value
With the G-T haplotype at rs 7007329-rs8178750	5	1	11.4	1.32–97.9	0.013*
Others	177	402	1	–	–

IS, ischemic stroke; controls, non-ischemic stroke subjects; OR, odds ratio; 95% CI, 95% confidence interval; Others, without the G-T haplotype; p-value was obtained from the Fisher's exact test; *significant difference.

identifying and locating complex disease genes. Some specific haplotype combinations in functional regions such as promoters or exons affect disease genesis (23). Positions of some susceptibility genes of multifactorial diseases have been identified using haplotype analysis (24, 25). Several association studies based on the distribution of haplotypes derived from genotypes have been performed (26, 27).

The power of the above-mentioned haplotype analysis is dependent upon the LD between the relevant SNPs. The LD analysis for all possible two-way comparisons among SNPs finds both a strong LD and a weak LD block when using several widely employed methods (D, D′, and r^2) (18, 19). The LD pattern, as well as the significance of the LD between all of the SNP combinations, showed the often observed block pattern in the genome, which can be explained by the existence of a few common haplotypes that account for most of the haplotype diversity (28). Based on such findings, we hypothesized that haplotype and LD analysis would be useful for assessing association between haplotypes and IS, resulting in the present attempt to establish haplotypes of the tPA gene consisting of SNPs. In the present genotype study, we did not observe any statistically significant difference in the distribution of the individual SNPs between the IS and control subjects. However, LD analysis suggested that the SNP1-SNP3 combination was important in the performance of the haplotype-based case-control study, and a haplotype was significantly greater in the IS group than in the control group.

This study did not attempt to correlate significant haplotypes with plasma levels of tPA. Recent studies have investigated whether plasma levels of tPA were associated with polymorphism in the tPA gene in healthy subjects (29). Since all five SNPs employed in our study were located in the intron, they were thought not to be functional. Even though the G-T haplotype at rs7007329-rs8178750 is not functional, it might be linked to the functional mutation that is involved in the pathophysiological role for IS. The diplotype analysis we performed also supports this hypothesis.

In conclusion, the G-T haplotype at rs7007329-rs8178750 of the human tPA gene may be used as a genetic marker for IS, and the haplotype may linked to a possible mutation in the tPA or neighboring genes.

Acknowledgements

This work was supported by a grant from the Ministry of Education, Science and Culture of Japan (High-Tech Research Center, Nihon University). We would like to thank Ms. K. Sugama for her excellent technical assistance.

References

1. Hassan A, Markus HS. Genetics and ischaemic stroke. Brain 2000; 123: 1784–812.
2. Rubattu S, Di Angelantonio E, Nitsch D, et al. Polymorphisms in prothrombotic genes and their impact on ischemic stroke in a Sardinian population. Thromb Haemost 2005; 93: 1095–100.
3. Ridker PM, Hennekens CH, Stampfer MJ, et al. Prospective study of endogenous tissue plasminogen activator and risk of stroke. Lancet 1994; 343: 940–3.
4. Pizzo SV, Petruska DB, Doman KA, et al. Releasable vascular plasminogen activator and thrombotic strokes. Am J Med 1985; 79: 407–11.
5. Ridker PM, Vaughan DE, Stampfer MJ, et al. Endogenous tissue-type plasminogen activator and risk of myocardial infarction. Lancet 1993; 341: 1165–8.
6. ECAT Angina Pectoris Study Group. ECAT angina pectoris study: baseline associations of haemostatic factors with extent of coronary arteriosclerosis and other coronary risk factors in 3000 patients with angina pectoris undergoing coronary angiography. Eur Heart J 1993; 14: 8–17.
7. Jansson JH, Nilsson TK, Olofsson BO. Tissue plasminogen activator and other risk factors as predictors of cardiovascular events in patients with severe angina pectoris. Eur Heart J 1991; 12: 157–61.
8. Degen SJ, Rajput B, Reich E. The human tissue plasminogen activator gene. J Biol Chem 1986; 25: 6972–85.
9. Jannes J, Hamilton-Bruce MA, Pilotto L, et al. Tissue plasminogen activator -7351C/T enhancer polymorphism is a risk factor for lacunar stroke. Stroke 2004; 35: 1090–4.
10. Nakayama T, Asai S, Sato N, et al. Genotype and haplotype association study of the STRK1 region on 5q12 among Japanese: a case-control study. Stroke 2006; 37: 69–76.
11. Sano M, Kuroi N, Nakayama T, et al. Association study of calcitonin-receptor-like receptor gene in essential hypertension. Am J Hypertens 2005; 18: 403–8.
12. Nakayama T, Soma M, Kanmatsuse K, et al. The microsatellite alleles on chromosome 1 associated with essential hypertension and blood pressure levels. J Hum Hypertens 2004; 18: 823–8.
13. Zhang W, Collins A, Morton NE. Does haplotype diversity predict power for association mapping of disease susceptibility? Hum Genet 2004; 115: 157–64.
14. Nakayama T, Soma M, Sato N, et al. An association study in essential hypertension using functional polymorphisms in lymphotoxin-α gene. Am J Hypertens 2004; 17: 1045–9.
15. Dempster AP, Laird NM, Rubin DB. Maximum likelihood from in complete data via the EM algorithm. J R Stat Soc 1977; 39: 1–22.
16. Hasimu B, Nakayama T, Mizutani Y, et al. Haplotype analysis of the Human Renin Gene and Essential Hypertension. Hypertension 2003; 41: 308–12.
17. Nakayama T, Soma M, Takahashi Y, et al. Association analysis of CA repeat polymorphism of the endothelial nitric oxide synthase gene with essential hypertension in Japanese. Clin Genet 1997; 51: 26–30.
18. Lewontin RC. On measures of gametic disequilibrium. Genetics 1988; 120: 849–52.
19. Taillon-Miller P, Bauer-Sardina I, Saccone NL, et al. Juxtaposed regions of extensive and minimal linkage disequilibrium in human Xq25 and Xq28. Nat Genet 2000; 25: 324–8.
20. Rubattu S, Volpe M, Kreutz R, et al. Chromosomal mapping of quantitative trait loci contributing to stroke in a rat model of complex human disease. [Comment]. Nat Genet 1996; 13: 429–34.
21. Jood K, Ladenvall P, Tjarnlund-Wolf A, et al. Fibrinolytic gene polymorphism and ischemic stroke. Stroke 2005; 36: 2077–81.
22. Morris RW, Kaplan NL. On the advantage of haplotype-analysis in the presence of multiple disease-susceptibility alleles. Genet Epidemiol 2002; 23: 221-33.
23. Joosten PH, Toepoel M, Mariman EC, et al. Promoter haplotype combinations of the platelet-derived growth factor alpha-receptor gene predispose to human neural tube defects. Nat Genet 2001; 27: 215–7.
24. Sharma P, Hingorani A, Jia H, et al. Quantitative association between a newly identified molecular variant in the endothelin-2 gene and human essential hypertension. J Hypertens 1999; 7: 1281–7.
25. Ombra MN, Forabosco P, Casula S, et al. Identification of a new candidate locus for uric acid nephrolithiasis. Am J Hum Genet 2001; 68: 1119–29.
26. Hasimu B, Nakayama T, Mizutani Y, et al. A novel variable number of tandem repeat polymorphism of the renin gene and essential hypertension. Hypertens Res 2003; 26: 473–7.
27. Kumar NN, Benjafield AV, Lin RC, et al. Haplotype analysis of aldosterone synthase gene (CYP11B2) polymorphisms shows association with essential hypertension. J Hypertens 2003; 21: 1331–7.
28. Gabriel SB, Schaffner SF, Nguyen H, et al. The structure of haplotype blocks in the human genome. Science 2002; 296: 2225–9.
29. Ladenvall P, Nilsson S, Jood K, et al. Genetic variation at the human tissue-type plasminogen activator (tPA) locus: haplotypes and analysis of association to plasma levels of tPA. Eur J Hum Genet 2003; 11: 603–10.

THE JOURNAL OF BIOLOGICAL CHEMISTRY VOL. 281, NO. 50, pp. 38489–38497, December 15, 2006

Involvement of GSK-3β and DYRK1B in Differentiation-inducing Factor-3-induced Phosphorylation of Cyclin D1 in HeLa Cells*

Received for publication, May 31, 2006, and in revised form, September 21, 2006 Published, JBC Papers in Press, October 17, 2006, DOI 10.1074/jbc.M605205200

Fumi Takahashi-Yanaga[‡1], Jun Mori[‡], Etsuko Matsuzaki[‡], Yutaka Watanabe[§], Masato Hirata[¶], Yoshikazu Miwa[‡], Sachio Morimoto[‡], and Toshiyuki Sasaguri[‡]

From the [‡]Department of Clinical Pharmacology, Faculty of Medical Sciences, Kyushu University, Fukuoka 812-8582, the [§]Department of Applied Chemistry, Faculty of Engineering, Ehime University, Matsuyama 790-8577, and the [¶]Department of Molecular and Cellular Biochemistry, Faculty of Dental Sciences, Kyushu University, Fukuoka 812-8582, Japan

Differentiation-inducing factors (DIFs) are putative morphogens that induce cell differentiation in *Dictyostelium discoideum*. We previously reported that DIF-3 activates glycogen synthase kinase-3β (GSK-3β), resulting in the degradation of cyclin D1 in HeLa cells. In this study, we investigated the effect of DIF-3 on cyclin D1 mutants (R29Q, L32A, T286A, T288A, and T286A/T288A) to clarify the precise mechanisms by which DIF-3 degrades cyclin D1 in HeLa cells. We revealed that T286A, T288A, and T286A/T288A mutants were resistant to DIF-3-induced degradation compared with wild-type cyclin D1, indicating that the phosphorylation of Thr^{286} and Thr^{288} were critical for cyclin D1 degradation induced by DIF-3. Indeed, DIF-3 markedly elevated the phosphorylation level of cyclin D1, and mutations introduced to Thr^{286} and/or Thr^{288} prevented the phosphorylation induced by DIF-3. Depletion of endogenous GSK-3β and dual-specificity tyrosine phosphorylation regulated kinase 1B (DYRK1B) by RNA interference attenuated the DIF-3-induced cyclin D1 phosphorylation and degradation. The effect of DIF-3 on DYRK1B activity was examined and we found that DIF-3 also activated this kinase. Further, we found that not only GSK-3β but also DYRK1B modulates cyclin D1 subcellular localization by the phosphorylation of Thr^{288}. These results suggest that DIF-3 induces degradation of cyclin D1 through the GSK-3β- and DYRK1B-mediated threonine phosphorylation in HeLa cells.

Differentiation-inducing factors (DIFs),[2] first identified in *Dictyostelium discoideum* as putative morphogens required for stalk cell differentiation (1, 2), also affect mammalian cells. In the DIF family (DIF-1, DIF-2, and DIF-3), DIF-3 (1-(3-chloro-2,6-dihydroxy-4-methoxyphenyl)-1-hex-anone) is the most potent inhibitor of proliferation in mammalian cells (3). However, the target molecule of DIFs is unknown, even in *Dictyostelium*. Although Shimizu *et al.* (4) recently reported that calmodulin-dependent cyclic nucleotide phosphodiesterase (PDE1) could be a pharmacological target molecule for DIF-1, specific inhibitor for PDE1 failed to mimic the antiproliferative effect of DIF-1. We reported that DIF-1 and/or DIF-3 inhibited mammalian cell proliferation by suppressing the expression of cyclin D1 via the activation of glycogen synthase kinase-3β (GSK-3β) (5–8). However, the precise mechanisms underlying cyclin D1 degradation induced by DIFs are not yet known.

Cyclin D1 is synthesized in the early G_1 phase and plays a key role in the initiation and progression of this phase (9, 10). There is a destruction box-like motif in the N terminus, which is required for cyclin D1 degradation induced by genotoxic stress (11). The expression level of cyclin D1 is regulated by ubiquitin-dependent mechanism, which is triggered by the phosphorylation of threonine residues located near the carboxyl terminus of cyclin D1 (12). Diehl *et al.* (13) reported that GSK-3β phosphorylates cyclin D1 on Thr^{286}, thereby stimulating cyclin D1 turnover in response to mitogenic signals. According to the model they proposed, cyclin D1 phosphorylation on Thr^{286} by GSK-3β induces the exclusion of cyclin D1 from nucleus to initiate its proteasomal degradation. Recently, Zou *et al.* (14) reported that dual-specificity tyrosine phosphorylation regulated kinase 1B (DYRK1B), a member of the DYRK family, phosphorylates cyclin D1 on Thr^{288}, also resulting in its degradation.

GSK-3β, a member of the Wnt signaling pathway, is a serine/threonine kinase involved in a variety of cellular processes. Although GSK-3β is a cytosolic protein, it is translocated into the nucleus when activated (15–17). DYRK1B, also a serine/threonine kinase found in nucleus (18), is highly expressed in normal skeletal muscle and certain carcinoma cell lines, including HeLa cells, and is not detectably expressed in many normal tissues (19). There are some similarities between GSK-3β and DYRK1B, because they phosphorylate the same substrates (glycogen synthase and cyclin D1) (14, 20).

In this study, we investigated the effect of DIF-3 on cyclin D1 and found that the threonine residues, but not the destruction box-like motif, play a key role in cyclin D1 degradation induced

* This work was supported by grants from the Ministry of Education, Culture, Sports, Science and Technology (a grant-in-aid for Scientific Research). The costs of publication of this article were defrayed in part by the payment of page charges. This article must therefore be hereby marked "*advertisement*" in accordance with 18 U.S.C. Section 1734 solely to indicate this fact.

[1] To whom correspondence should be addressed: Dept. of Clinical Pharmacology, Faculty of Medical Sciences, Kyushu University, Fukuoka 812-8582, Japan. Tel.: 81-92-642-6082; Fax: 81-92-642-6084; E-mail: yanaga@clipharm.med.kyushu-u.ac.jp.

[2] The abbreviations used are: DIF, differentiation-inducing factor; GSK-3β, glycogen synthase kinase-3β; DYRK1B, dual-specificity tyrosine phosphorylation-regulated kinase 1B; PDE1, calmodulin-dependent cyclic nucleotide phosphodiesterase; ALLN, *N*-acetyl-Leu-Leu-Norleucinal; MKK3, mitogen-activated protein kinase kinase 3; RNAi, RNA interference; IKKα, IκB kinase α; MAPK, mitogen-activated protein kinase; MBP, myelin basic protein.

by DIF-3 in HeLa cells. Moreover, we revealed that not only GSK-3β but also DYRK1B was involved in the phosphorylation of cyclin D1 induced by DIF-3 in HeLa cells. Thus DIF-3 efficiently induced degradation of cyclin D1.

EXPERIMENTAL PROCEDURES

Chemicals—DIF-3 (1-(3-chloro-2, 6-dihydroxy-4-methoxyphenyl)-1-hexanone) was synthesized according to Masento *et al.* (21). SB216763 was purchased from BIOMOL international. The monoclonal anti-β-actin antibody, anti-FLAG M2 antibody, and *N*-acetyl-Leu-Leu-norleucinal (ALLN) were from Sigma. Polyclonal anti-cyclin D1 antibody was from Santa Cruz Biotechnology. Monoclonal anti-GAPDH antibody was from Abcam. Polyclonal anti-DYRK1B antibody was from ABGENT. Monoclonal anti-histone H3 antibody was from Upstate Biotechnology.

Cell Culture and Transfection—HeLa cells were grown in Dulbecco's modified Eagle's medium (Sigma) supplemented with 10% fetal bovine serum, 100 units/ml penicillin G, and 100 μg/ml streptomycin. The wild-type human cyclin D1 cDNA was subcloned into pcDNA3 (Invitrogen) as described previously (6). Human cyclin D1 mutants R29Q, L32A, T286A, T288A, and T286A/T288A were generated by a QuikChange® Site-directed Mutagenesis kit (Stratagene). The FLAG-tagged human cyclin D1 constructs were also generated. Human cyclin D1 pGL3 basic luciferase reporter construct was a generous gift from Drs. O. Tetsu and F. McCormick, University of California San Francisco. Transfection was carried out using Lipofectamine™Plus transfection reagent (Invitrogen).

RNA Interference (RNAi)—GSK-3β validated Stealth™ RNAi was purchased from Invitrogen. Double-stranded Stealth™ RNAi specifically targeting human DYRK1B (5′-gccugguauuugagcugcuguccua-3′) was synthesized (Invitrogen). Transfection of RNAi was carried out according to the manufacturer protocol using Lipofectamine™ 2000 transfection reagent (Invitrogen). Stealth™ RNAi negative controls, which are the GC-matched scrambled sequence, were also purchased from Invitrogen.

Western Blot Analysis—Samples were separated by 12% SDS-PAGE and transferred to a polyvinylidene difluoride membrane using a semi-dry transfer system (1 h, 12 V). After blocking with 5% skim milk for 1 h, the membrane was probed with a first antibody. The membrane was washed three times and incubated with horseradish peroxidase-conjugated anti-rabbit or anti-mouse IgG (Cell Signaling Technology) for 1 h. Immunoreactive proteins on the membrane were visualized by treatment with a detection reagent (LumiGLO, Cell Signaling Technology). An optical densitometric scan was performed using Science Lab 99 Image Gauge Software (Fuji Photo Film).

Luciferase Reporter Assay—HeLa cells were transfected with luciferase reporter plasmid and pRL-SV40, a *Renilla* luciferase expression plasmid (Toyo Ink Mfg Co) for the control of transfection efficiency. Cells were cultured for 24 h after transfection and stimulated with DIF-1 (30 μM) for 1 h. The luciferase activity was determined with a luminometer (Lumat LB 9507, Berthold Technologies) and normalized with respect to *Renilla* luciferase activity.

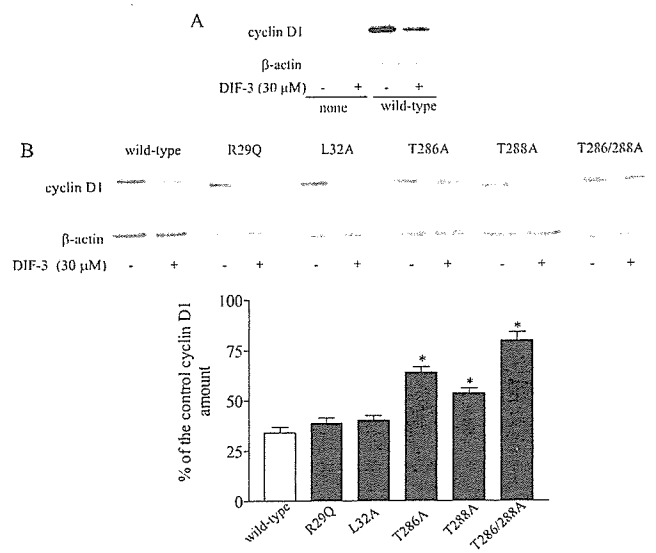

FIGURE 1. **The effect of cyclin D1 mutations on DIF-3-induced degradation.** *A*, comparison of the intrinsic cyclin D1 and overexpressed wild-type cyclin D1. *B*, effect of DIF-1 on cyclin D1 mutants. Cells were transfected with the plasmid containing indicated type of cyclin D1 for 7 h and were incubated with or without DIF-3 (30 μM) for 1 h. Protein samples were subjected to immunoblot analysis using the anti-cyclin D1 antibody. The levels of cyclin D1 amounts were quantified by densitometry and normalized to those of β-actin. The results are shown as percentages of cyclin D1 amounts in DIF-3-treated cells to those in control cells. Values are means ± S.E. of three independent experiments. *, $p < 0.01$, compared with the wild-type cyclin D1 (Student's *t* test).

^{32}P Metabolic Labeling and Immunoprecipitation—HeLa cells were preincubated in phosphate-free medium (Invitrogen) for 1 h and ALLN (20 μM) was added to prevent cyclin D1 degradation. Subsequently, cells were labeled with 100 μci/ml of [^{32}P]orthophosphate (PerkinElmer) for 1 h followed by stimulation with DIF-3. Cells were lysed on ice in the lysis buffer (150 mM NaCl, 5 mM NaF, 2 mM Na_3VO_4, 50 mM Tris/HCl, pH 7.4, 1 mM EDTA, 1% (v/v) Tween 20, and 2 mM phenylmethylsulfonyl fluoride) and insoluble cell debris was removed by centrifugation at 5000 rpm for 3 min. The cell lysate was precleared with protein G-Sepharose CL-4B (Amersham Biosciences) and then incubated with protein G-Sepharose CL-4B and an anti-cyclin D1 antibody or an anti-FLAG antibody (2 μg) at 4 °C for 3 h. After incubation, proteins bound to the antibody/protein G-Sepharose complex were precipitated by centrifugation at 15,000 rpm for 5 min and washed three times with the lysis buffer. The samples were denatured in SDS sample buffer and separated by 12% SDS-PAGE, followed by the transfer to a polyvinylidene difluoride membrane prior to autoradiography. The radioactive bands were quantified using Science Lab 99 Image Gauge Software (Fuji Photo Film). After autoradiography, the membrane was subjected to Western blot analysis for cyclin D1.

In Vitro DYRK1B Kinase Reaction—The *in vitro* kinase assay of DYRK1B was carried out according to Lim *et al.* (22). Briefly, cells were stimulated with or without DIF-3 and immunoprecipitation was carried out using 2 μg of anti-DYRK1B antibody. The immunoprecipitated samples were washed twice with lysis buffer and twice with a kinase assay buffer (20 mM Tris/HCl, pH 7.4, 5 mM $MgCl_2$, and 1 mM dithiothreitol). The kinase activities of DYRK1B were tested with 30 μl of kinase assay buffer con-

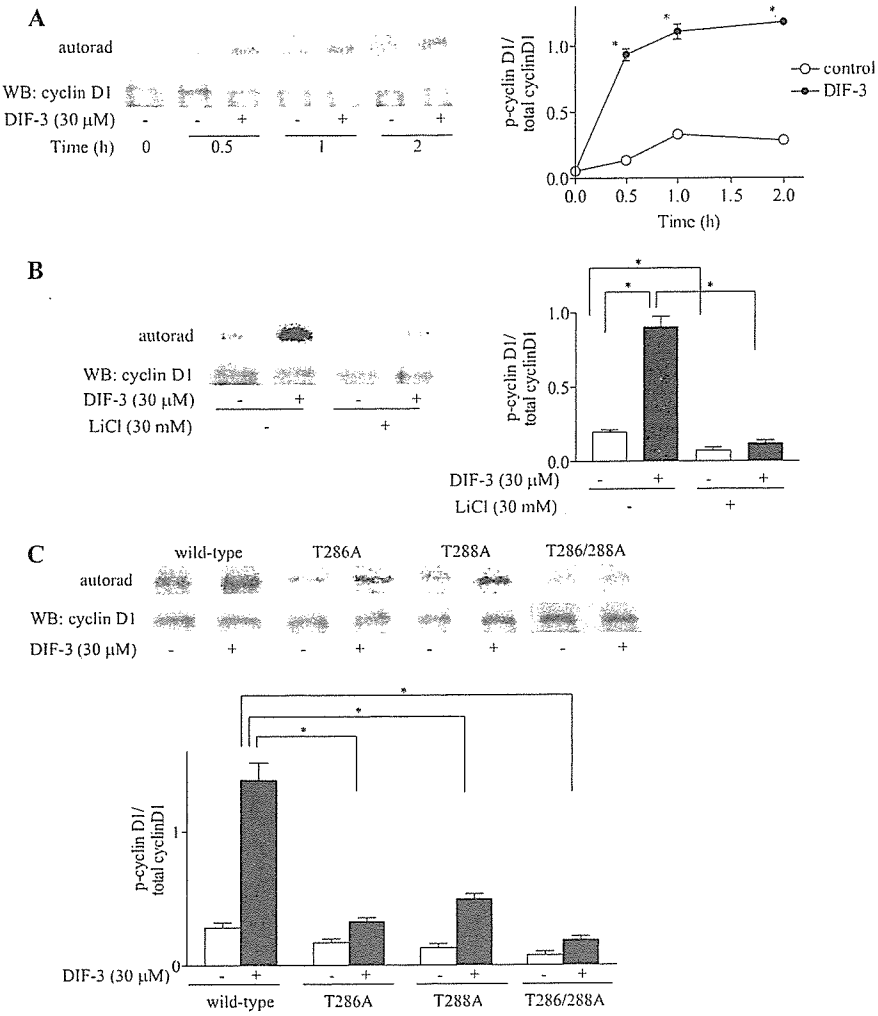

FIGURE 2. **DIF-3 induced phosphorylation on cyclin D1.** *A*, effect of DIF-1 on the time course of cyclin D1 phosphorylation. Cells were metabolically labeled with [^{32}P]orthophosphate in the presence of ALLN (20 μM) and stimulated with DIF-3 (30 μM) for the indicated periods. Samples were subjected to immunoprecipitation using anti-cyclin D1 antibody. After electrophoresis and transfer, phosphorylated-cyclin D1 was visualized by autoradiography. The membrane was then subjected to Western blot analysis for cyclin D1. The levels of radioactive bands and immunoreactive bands were quantified and the results are shown as ratios of phosphorylated cyclin D1 (*p-cyclin D1*) to cyclin D1 amount (*total cyclin D1*). Values are means ± S.E. of three independent experiments. *, $p < 0.01$, compared with the control (Student's *t* test). *B*, effect of LiCl. Cells were metabolically labeled with [^{32}P]orthophosphate in the presence of ALLN (20 μM) and LiCl (30 mM), followed by the stimulation with DIF-3 (30 μM) for 1 h. Values are means ± S.E. of three independent experiments. *, $p < 0.01$ compared with columns indicated (*t* test). *C*, effect of Thr^{286} and/or Thr^{288} mutation on cyclin D1 phosphorylation induced by DIF-3. Cells were transfected with the plasmid containing indicated type of cyclin D1. Transfected cells were metabolically labeled with [^{32}P]orthophosphate in the presence of ALLN (20 μM), followed by the stimulation with DIF-3 (30 μM) for 1 h. Values are means ± S.E. of three independent experiments. *, $p < 0.01$, compared with columns indicated (Student's *t* test).

taining 20 mM Tris/HCl (pH 7.4), 5 mM $MgCl_2$, 1 mM dithiothreitol, 250 μM ATP, 5 μCi of [γ-^{32}P]ATP (Amersham Biosciences), and 20 μg of myelin basic protein (MBP) from Upstate Biotechnology. The samples were incubated at 30 °C for 30 min, and the reaction was terminated by adding 10 μl of SDS sample buffer. Samples were then separated by 12% SDS-PAGE and the gel was stained with Coomassie Brilliant Blue R-250 prior to autoradiography. The radioactive bands were quantified using Science Lab 99 Image Gauge Software (Fuji Photo Film).

Flow Cytometry—Cells harvested by the trypsin/EDTA treatment were suspended in hypotonic fluorochrome solution containing 50 μg/ml of propidium iodide (PI), 0.1% sodium citrate, and 0.1% Triton X-100 (6). Cells (5×10^3) for each sample were analyzed for fluorescence by a Becton-Dickinson FACScalibur.

Purification of Nucleic Proteins—Nucleic proteins were purified from cells transfected with indicated plasmid using NE-PER™ nuclear and cytoplasmic extraction reagents (Pierce).

Fluorescence Microscopy—Cells plated on coverslips were transfected with FLAG-tagged cyclin D1 constructs. Immunofluorescence detection of FLAG-tagged cyclin D1 was performed as described previously using an anti-FLAG antibody (6).

RESULTS

Effect of DIF-3 on Cyclin D1 and Its Mutants—There are at least three independent motifs in cyclin D1 involved in its degradation. The first one is the Arg-*X*-*X*-Leu destruction box (Arg^{29}-*X*-*X*-Leu^{32}), which plays a major role in rendering cyclin D1 susceptible to degradation by ionizing radiation (11). The second one is Thr^{286}, which is phosphorylated by GSK-3β to induce cyclin D1 degradation (12, 13). The third one is Thr^{288}, recently identified by Zou *et al.* (14), who reported that a serine/threonine kinase DYRK1B phosphorylates cyclin D1 at Thr^{288}, also leading to the degradation of cyclin D1. Therefore, we investigated five different mutants of cyclin D1 (R29Q, L32R, T286A, T288A, and T286A/T288A) to determine the mechanisms by which DIF-3 induces cyclin D1 degradation in HeLa cells. As shown in Fig. 1*A*, the effect of DIF-3 on overexpressed wild-type cyclin D1 was similar to the effect on intrinsic cyclin D1. While R29Q and L32R mutants were fully responsive to DIF-3, T286A, T288A, and T286A/T288A mutations significantly reduced the effect of DIF-3 (Fig. 1*B*). Among these three mutations, T286A/T288A most strongly resisted DIF-3. These results suggest that the phosphorylation of both Thr^{286} and Thr^{288} were critical for DIF-3-induced cyclin D1 degradation. To analyze the effect of DIF-3 on cyclin D1 promoter activity, we performed luciferase reporter assay using the human cyclin D1 promoter construct pGL3-basic vector (8). However, DIF-3 did not have significant effect on promoter activity after 1 h incubation (440757.8 ±

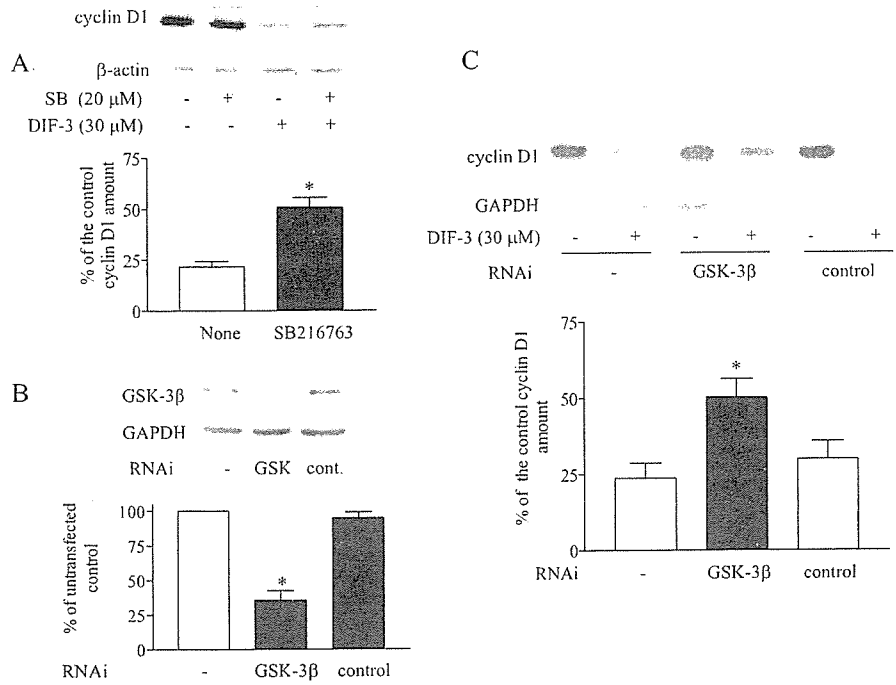

FIGURE 3. **Inhibition and depletion of GSK-3β prevented the degradation of cyclin D1 induced by DIF-3.** *A*, the effect of GSK-3β inhibitor, SB216763. HeLa cells were pretreated with or without SB216763 (20 μM) for 3 h and then incubated in the presence or absence of DIF-3 (30 μM) for 1 h. Protein samples were separated by 12% SDS-PAGE and immunoblotted for cyclin D1. The expression levels of cyclin D1 were quantified by densitometry and normalized to those of β-actin. The results are shown as percentages of cyclin D1 amounts in DIF-3-treated cells to those in control cells. Values are means ± S.E. of three independent experiments. *, $p < 0.01$ compared with the minus inhibitor (Student's *t* test). *B*, depletion of GSK-3β by RNAi. Cells were transfected with control RNAi or RNAi to GSK-β (100 nM). Protein samples were subjected to immunoblot analysis using the anti-GSK-3β antibody. The expression levels of GSK-3β were quantified by densitometry and normalized to those of GAPDH. Values are means ± S.E. of three independent experiments. *, $p < 0.05$ compared with the minus RNAi (Student's *t* test). *C*, depletion of GSK-3β by RNAi attenuated the effect of DIF-1. Cells were transfected with control RNAi or RNAi to GSK-3β (100 nM) and were incubated with or without DIF-3 (30 μM) for 1 h. Protein samples were subjected to immunoblot analysis using the anti-cyclin D1 antibody. The expression levels of cyclin D1 were quantified by densitometry and normalized to those of GAPDH. The results are shown as percentages of cyclin D1 amounts in DIF-3-treated cells to those in control cells. Values are means ± S.E. of three independent experiments. *, $p < 0.05$ compared with the minus RNAi (Stduent's *t* test).

15929.4 (mean ± S.E., $n = 6$) for control cells and 425032.3 ± 10135.5 (mean ± S.E., $n = 6$) for DIF-3-treated cells). This result is consistent with our previous report (6) which showed that DIF-3 reduced cyclin D1 mRNA amount after 3 h incubation. Because cells were treated with DIF-3 for 1 h to analyze the effect of DIF-3 on cyclin D1 mutants, we concluded that the reduction of cyclin D1 protein amount was caused by the protein degradation induced by DIF-3.

DIF-3-phosphorylated Cyclin D1 at Thr^{286} and Thr^{288}—We subsequently examined whether DIF-3 induces the phosphorylation of cyclin D1 in intact cells. We have previously reported that ALLN, which inhibits ubiquitin-proteasome-dependent degradation of cyclins, prevented the DIF-3-induced cyclin D1 degradation in HeLa cells. Therefore, cells were pretreated with ALLN to avoid cyclin D1 degradation induced by DIF-3 and metabolically labeled with [^{32}P]orthophosphate. Cyclin D1 was immunoprecipitated for analysis by autoradiography and immunoblotting. By the immunoprecipitation, 51.3 ± 4.5% (mean ± S.E., $n = 3$) of cyclin D1 was cleared from the lysate. As shown in Fig. 2*A*, DIF-3 induced phosphorylation of cyclin D1 in a time-dependent manner. Pretreatment with LiCl, which inhibits GSK-3β, prevented the phosphorylation of cyclin D1 induced by DIF-3 (Fig. 2*B*). To determine whether Thr^{286} and Thr^{288} residues are involved in DIF-3-induced cyclin D1 phosphorylation, mutated cyclin D1 proteins (T286A, T288A and T286A/T288A) were overexpressed in HeLa cells. The effect of DIF-1 was greatly attenuated in the T286A mutant and significantly reduced in the T288A cyclin D1 mutant (Fig. 2*C*). T286A/T288A double mutation almost completely abolished the phosphorylation induced by DIF-3. This result was well correlated with the result shown in Fig. 1*B*. Thus, DIF-3 seemed to induce cyclin D1 phosphorylation at Thr^{286} and Thr^{288}, triggering cyclin D1 degradation.

Inhibition of GSK-3β Attenuated DIF-3-induced Cyclin D1 Degradation—We previously reported that DIF-3 activated GSK-3β and induced cyclin D1 degradation by the acceleration of ubiquitin-proteasome-dependent proteolysis in HeLa cells (6). To elucidate the role of GSK-3β in DIF-3-induced cyclin D1 degradation, HeLa cells were pretreated with SB216763, a specific GSK-3α and β inhibitor. As shown in Fig. 3*A*, although SB216763 (20 μM) attenuated the degradation of cyclin D1 induced by DIF-3, this compound could not fully inhibit DIF-3 action, even if this concentration of SB216763 caused complete inhibition of GSK-3β activity in *in vitro kinase assay* using phospho-Glycogen Synthase Peptide-2 (Upstate Biotechnology) as substrate (data not shown). Subsequently, we attempted to deplete endogenous GSK-3β using RNAi to determine the involvement of GSK-3β in DIF-3 action. As shown in Fig. 3*B*, the protein level of GSK-3β was markedly reduced by transfection with GSK-3β RNAi. The depletion of GSK-3β by transfection with GSK-3β RNAi attenuated the effect of DIF-3 on cyclin D1 degradation, while control RNAi (GC-matched scrambled sequence) did not have a significant effect (Fig. 3*C*). These results clearly indicated the involvement of GSK-3β in the DIF-3-induced cyclin D1 degradation but GSK-3β was unlikely to be the only kinase responsible for cyclin D1 degradation induced by DIF-3.

Depletion of DYRK1B Attenuated the Cyclin D1 Degradation Induced by DIF-3—Recently, it has been reported that DYRK1B phosphorylates cyclin D1 at Thr^{288} leading to the proteolysis of cyclin D1 (14). Because DIF-3 induced phosphorylation of Thr^{288}, the involvement of DYRK1B in the DIF-3-induced degradation of cyclin D1 was investigated. For this purpose, endogenous DYRK1B was depleted with RNAi. As shown in Fig. 4*A*, the protein level of DYRK1B was markedly reduced by trans-

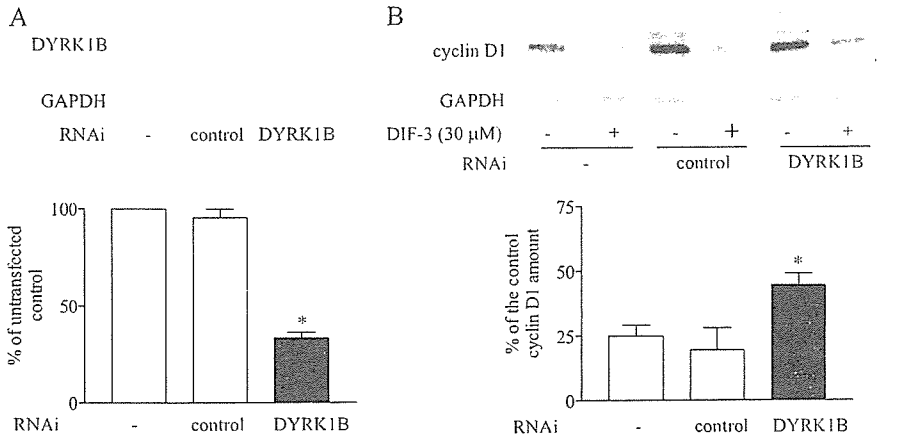

FIGURE 4. **Depletion of DYRK1B prevented the degradation of cyclin D1 induced by DIF-3.** *A*, depletion of DYRK1B by RNAi. Cells were transfected with control RNAi or RNAi to DYRK1B (100 nM). Protein samples were subjected to immunoblot analysis using the anti-DYRK1B antibody. The expression levels of DYRK1B were quantified by densitometry and normalized to those of GAPDH. Values are means ± S.E. of three independent experiments. *, $p < 0.05$ compared with the minus RNAi (Student's *t* test). *B*, depletion of DYRK1B by RNAi attenuated the effect of DIF-1. Cells were transfected with control RNAi or RNAi to DYRK1B (100 nM) and were incubated with or without DIF-3 (30 μM) for 1 h. Protein samples were subjected to immunoblot analysis using the anti-cyclin D1 antibody. The expression levels of cyclin D1 were quantified by densitometry and normalized to those of GAPDH. The results are shown as percentages of cyclin D1 amounts in DIF-3-treated cells to those in control cells. Values are means ± S.E. of three independent experiments. *, $p < 0.05$ compared with the minus RNAi (Student's *t* test).

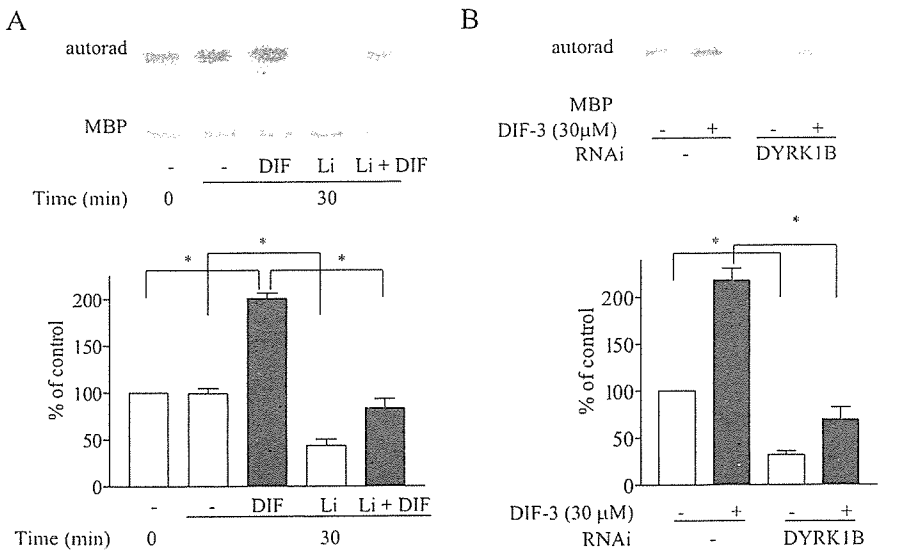

FIGURE 5. **DYRK1B was activated by DIF-3.** *A*, DIF-3 activated DYRK1B. Cells were pretreated with or without LiCl (30 mM) and stimulated with DIF-3 (30 μM) for 30 min. DYRK1B was immunoprecipitated and subjected to *in vitro* kinase assay using MBP as substrate in the presence or absence of LiCl. The levels of radioactive bands were quantified by densitometry and normalized to the levels of MBP. Values are means ± S.E. of three independent experiments. *, $p < 0.01$, compared with the columns indicated (Student's *t* test). *B*, inhibition of DYRK1B activity by RNAi. Cells were transfected with RNAi to DYRK1B (100 nM) and stimulated with DIF-3 (30 μM) for 30 min. DYRK1B was immunoprecipitated and subjected to *in vitro* kinase assay. Values are means ± S.E. of three independent experiments. *, $p < 0.01$, compared with the columns indicated (Student's *t* test).

fection with DYRK1B RNAi. Although the control RNAi (GC matched scrambled sequence) did not have a significant effect, the depletion of DYRK1B significantly attenuated the effect of DIF-1 on cyclin D1 degradation (Fig. 4*B*), suggesting the involvement of DYRK1B in cyclin D1 degradation induced by DIF-3.

DIF-3 Activated DYRK1B—To clarify the effect of DIF-3 on DYRK1B activity, *in vitro* kinase assay was carried out using MBP as substrate (22). HeLa cells were stimulated with or without DIF-3 for 30 min and DYRK1B was immunoprecipitated to subject to kinase assay. As shown in Fig. 5*A*, DIF-3 significantly activated DYRK1B by 200% of control after 30 min incubation. Since LiCl almost completely inhibited cyclin D1 phosphorylation induced by DIF-3, the effect of LiCl on DYRK1B activity was examined. Interestingly, LiCl also attenuated the DYRK1B activity but failed to complete inhibition of this kinase (Fig. 5*A*). This result was agreeable with previous report which observed that LiCl strongly inhibit GSK-3β and weakly but significantly attenuated DYRK1B (14). We subsequently examined the effect of DYRK1B RNAi. As shown in Fig. 5*B*, DYRK1B RNAi markedly reduced the kinase activity to 30% of control and this reduction was well correlated with the reduction of DYRK1B protein level by RNAi shown in Fig. 4*A*.

GSK-3β and DYRK1B Phosphorylated Thr^{286} and Thr^{288} on Cyclin D1, Respectively, and Modified Cyclin D1 Subcellular Localization—Next, we examined the effect of depletion of GSK-3β and DYRK1B on cyclin D1 phosphorylation induced by DIF-3. As shown in Fig. 6*A*, the depletion of GSK-3β or DYRK1B significantly reduced but did not abolish the cyclin D1 phosphorylation induced by DIF-3. Subsequently, we examined the effect of depletion of GSK-3β or DYRK1B on phosphorylation of cyclin D1 mutants to clarify which site(s) on cyclin D1, Thr^{286} or Thr^{288}, are phosphorylated by GSK-3β or DYRK1B. For this experiment, we used FLAG-tagged wild-type and mutated cyclin D1 expression vectors. Fig. 6*B* showed that DIF-3 failed to induce phosphorylation on T288A cyclin D1 mutant after GSK-3β depletion. On the other hand, T286A cyclin D1 mutant was not significantly phosphorylated by DIF-3 treatment after depletion of DYRK1B. These results suggested that Thr^{286} was phosphorylated by GSK-3β and Thr^{288} was phosphorylated by DYRK1B, similarly to the previous reports (13, 14). We further examined the subcellular localization of wild-type and mutant cyclin D1. As shown in Fig. 6*C* and *D*, FLAG-tagged T286A and T288A cyclin D1 mutants were abundant in nucleus compared with wild-type. DIF-3

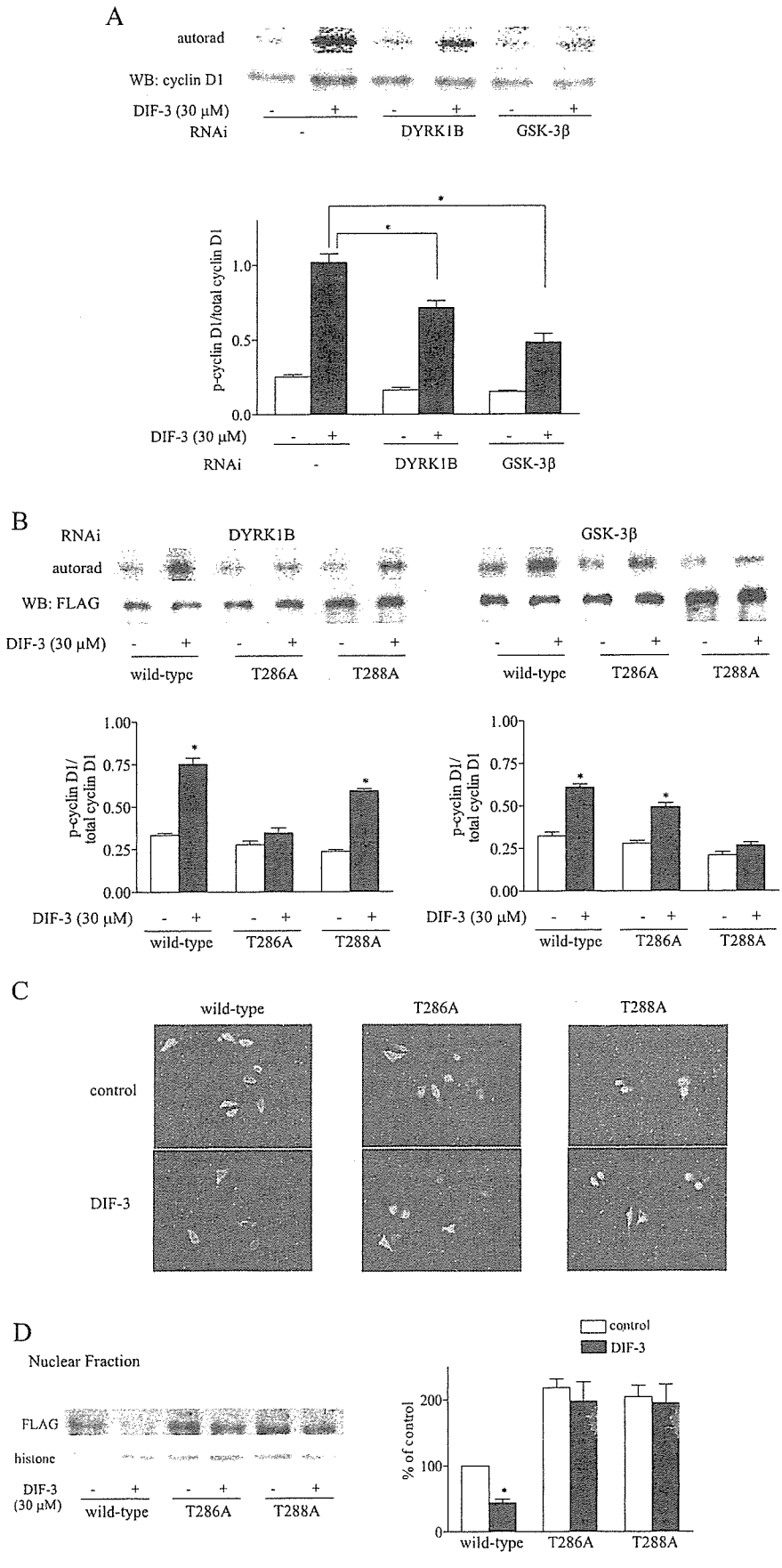

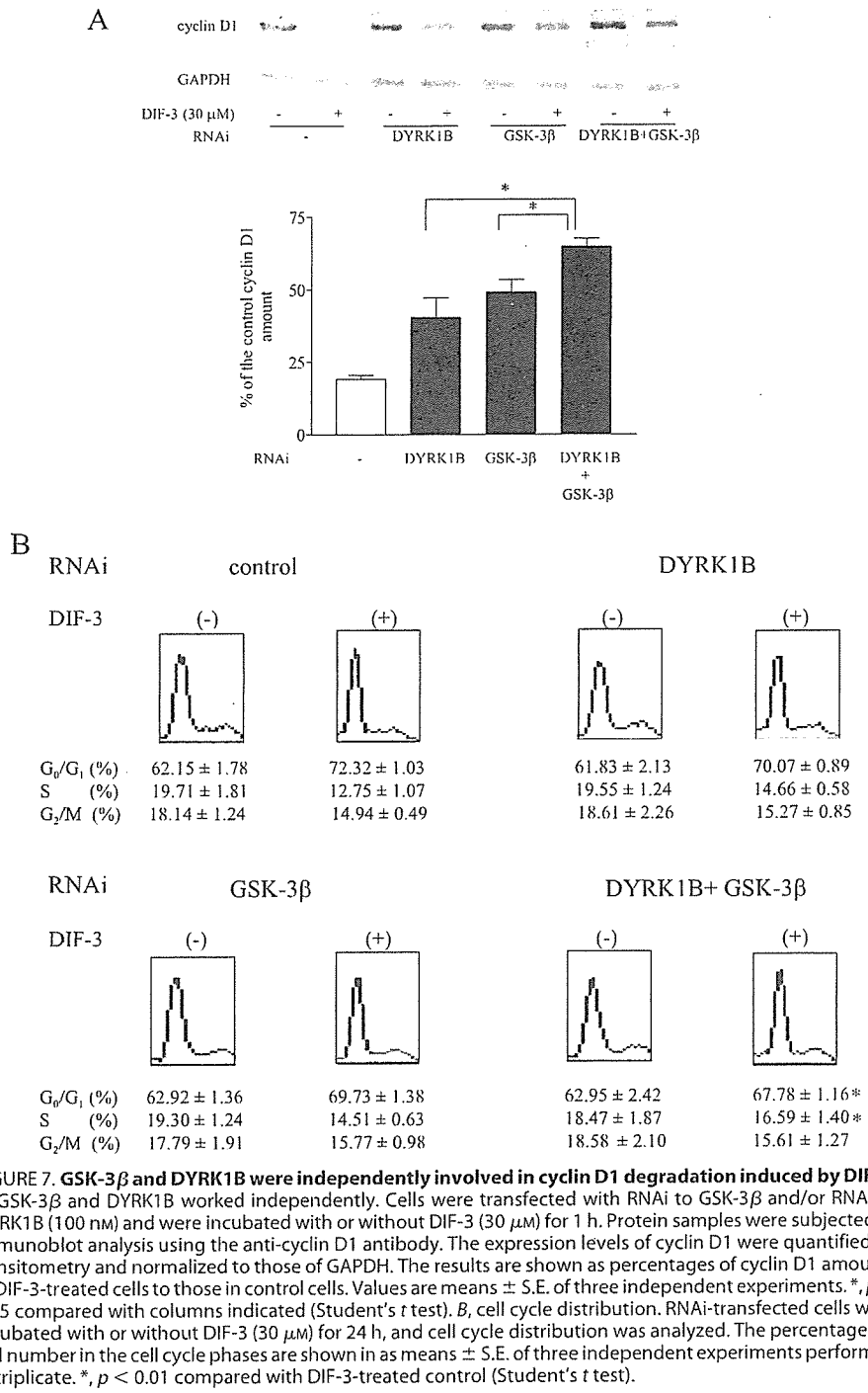

FIGURE 7. **GSK-3β and DYRK1B were independently involved in cyclin D1 degradation induced by DIF-3.** *A*, GSK-3β and DYRK1B worked independently. Cells were transfected with RNAi to GSK-3β and/or RNAi to DYRK1B (100 nM) and were incubated with or without DIF-3 (30 μM) for 1 h. Protein samples were subjected to immunoblot analysis using the anti-cyclin D1 antibody. The expression levels of cyclin D1 were quantified by densitometry and normalized to those of GAPDH. The results are shown as percentages of cyclin D1 amounts in DIF-3-treated cells to those in control cells. Values are means ± S.E. of three independent experiments. *, $p < 0.05$ compared with columns indicated (Student's *t* test). *B*, cell cycle distribution. RNAi-transfected cells were incubated with or without DIF-3 (30 μM) for 24 h, and cell cycle distribution was analyzed. The percentages of cell number in the cell cycle phases are shown in as means ± S.E. of three independent experiments performed in triplicate. *, $p < 0.01$ compared with DIF-3-treated control (Student's *t* test).

induced export of wild-type cyclin D1 from the nucleus, whereas T286A and T288A mutations significantly reduced the effect of DIF-3, suggesting that not only Thr^{286} but also Thr^{288} plays an important role to modulate the subcellular localization of cyclin D1. Taken together, Thr^{286} and Thr^{288} were likely to be phosphorylated by GSK-3β and DYRK1B, respectively, and subcellular localization of cyclin D1 seemed to be modulated by GSK-3β and DYRK1B.

GSK-3β and DYRK1B Were Independently Involved in Cyclin D1 Degradation Induced by DIF-3—Furthermore, to investigate the relationship between GSK-3β and DYRK1B in DIF-3 action, RNAi of GSK-3β and DYRK1B were co-transfected. As shown in Fig. 7*A*, co-transfection of GSK-3β and DYRK1B RNAis exhibited an additive effect for cyclin D1 degradation, suggesting that GSK-3β and DYRK1B independently induce the phosphorylation and the degradation of cyclin D1. Because we previously reported that cyclin D1 depletion is associated with cell cycle arrest following exposure to DIF-3 (6), we examined the effects of reduction of GSK-3β and/or DYRK1B on DIF-3-induced cell cycle arrest. Although transfection of GSK-3β or DYRK1B RNAi did not have a significant effect on the DIF-3-induced increase in the number of G_0/G_1 cells, co-transfection of GSK-3β and DYRK1B RNAis significantly attenuated the effect of DIF-3 (Fig. 7*B*). This result indicated that GSK-3β and DYRK1B played important roles in cell cycle arrest induced by DIF-3 in HeLa cells.

FIGURE 6. **DYRK1B and GSK-3β phosphorylated Thr^{288} and Thr^{286}, respectively, and modulated cyclin D1 localization.** *A*, depletion of GSK-3β and DYRK1B attenuated the phosphorylation of cyclin D1 induced by DIF-3. Cells were transfected with RNAi to GSK-3β or RNAi to DYRK1B (100 nM) and metabolically labeled with [^{32}P]orthophosphate in the presence of ALLN (20 μM), followed by the stimulation with DIF-3 (30 μM) for 1 h. The levels of radioactive bands and cyclin D1 amounts were quantified and the results are shown as ratios of phosphorylated cyclin D1 (*p-cyclin D1*) to cyclin D1 amount (*total cyclin D1*). Values are means ± S.E. of three independent experiments. *, $p < 0.01$, compared with columns indicated (Student's *t* test). *B*, DYRK1B and GSK-3β phosphorylated Thr^{288} and Thr^{286}, respectively. Cells were transfected with the plasmid containing indicated type of FLAG-tagged cyclin D1 and metabolically labeled with [^{32}P]orthophosphate in the presence of ALLN (20 μM), followed by the stimulation with DIF-3 (30 μM) for 1 h. Values are means ± S.E. of three independent experiments. *, $p < 0.01$, compared with control (Student's *t* test). *C*, immunofluorescence. Cells were plated on coverslips and transfected with the plasmid containing indicated type of FLAG-tagged cyclin D1. After a 3-h incubation with or without DIF-3 (30 μM), immunofluorescent staining was performed with the monoclonal anti-FLAG antibody. The results are representative of three independent experiments. *D*, subcellular localization of cyclin D1. Transfected cells were incubated with or without DIF-3 (30 μM), and nuclear proteins were purified. Western blot analysis was carried out using the monoclonal anti-FLAG antibody. The expression levels of FLAG-tagged cyclin D1 were quantified by densitometry and normalized to those of histone H3. The results are shown as percentages of FLAG-tagged cyclin D1 amounts in wild-type cyclin D1-transfected cells. Values are means ± S.E. of three independent experiments. *, $p < 0.01$ compared with control (Student's *t* test).